Universidade de Brasília
Faculdade de Medicina
Laboratório Multidisciplinar de Pesquisa em Doença de Chagas

METILTIOADENOSINA FOSFORILASE DE *TRYPANOSOMA CRUZI*, UM ALVO POTENCIAL PARA QUIMIOTERAPIA DA DOENÇA DE CHAGAS, APRESENTA AMPLA ESPECIFICIDADE A SUBSTRATOS E ELEVADA ESTABILIDADE ESTRUTURAL

DAVID NEVES

Orientador: Prof. Dr. Jaime Martins de Santana

Co-orientador: Prof. Dra. Sônia Maria de Freitas

Tese apresentada ao programa de Pós-graduação em Patologia Molecular da Universidade de Brasília como requisito parcial à obtenção do título de Doutor em Patologia Molecular

Brasília, 2006

Trabalho desenvolvido no Laboratório Multidisciplinar de Pesquisa em Doença de Chagas, Universidade de Brasília, sob a orientação do Prof. Jaime Santana e no Laboratório Nacional de Luz Síncrotron, em Campinas. Este trabalho teve apoio financeiro da CAPES e CNPq.

DEDICATÓRIA

Dedico esta tese aos meus pais, Telma e Osvaldo, pela vida, amor e apoio incondicionais em mais essa etapa.

Aos meus queridos irmãos Thaís e Moisés pela paciência e incentivo diários.

AGRADECIMENTOS

Ao professor Jaime Santana, pela confiança depositada, dedicação diária e incentivo em galgar novos horizonte. Obrigado pelo exemplo de competência como pesquisador e orientador.

À professora Sônia Freitas pela oportunidade de enveredar pelo fascinante mundo da biofísica, acessibilidade e paciência de repetir conceitos por tantas vezes confundidos e sempre com a mesma energia.

Ao professor Antônio Teixeira, pela oportunidade de trabalho e exemplo de amor a investigação científica.

À Izabela, pelo acolhimento no LMPDC, amizade, "broncas" sempre construtivas e exemplo de persistência.

Às eternas amigas de trabalho, Danielle, Carol, Glória, Flávia, Mariana, Meire, Carla, Nadjar, Lina, Perla, Adriana e especialmente a Teresa Cristina.

À minoria do LMPDC, Thiago, Alessandro, Cléver e Rubens pela amizade.

À Ana de Cássia, Márcia, Miguel e Geraldo pelo apoio técnico, fundamental na realização desse trabalho.

Aos professores do LNLS Javier Medrano e João Alexandre pela ajuda na elaboração e realização dos trabalhos de biofísica e cristalização.

À minha ex-orientadora e amiga, Cláudia Renata, pelos primeiros passos na pesquisa, ensinamentos de vida e incentivo.

Aos amigos da UnB, Carla Tatiana, Daniela, Tainá, Patrícia, Regina, Claudiner e Eduardo.

Aos companheiros de longa data Carpes, Alves e Zakir pela amizade incondicional e sempre presente.

Ao imenso apoio da minha avó Catarina, assim como da tia Vitória, tia Leila e primos Gabriela e Lucas.

E principalmente à Máisa, meu amor, pelo carinho, interesse, apoio e companheirismo.

LISTA DE ABREVIATURAS

[θ]	Elipcidade média por resíduo
°C	Grau centígrado
Ado	Adenosina
Arg	Arginina
CD	Dicroísmo circular
cDNA	Acido desoxirribonucléico complementar
CDP	Citidia-difosfato
cm	centímetro
CTAB	Hexadecil-trimetilamonia
Da	Dalton
dAdo	Deoxi-adenosina
dGTP	Deoxi-guanidina-trifosfato
DNA	Ácido desoxirribonucléico
DTT	Ditiotreitol
g	Grama
Gnd-HCl	Hidrocloreto de guanidina
GTP	Guanidina-trifosfato
HEPES	Ácido (2-hidroxietil)-piperazina etanosulfônico
His	Histidina
IgG	Imuno-globulina G
IPTG	Isopropil-β-D-tiogalactopiranosídeo
kb	Kilobase
k_{cat}	Constante catalítica
k_{cat}/K_m	Eficiência catalítica
K_m	Constante de Michaelis-Menten
K_u	Constante de equilíbrio do processo de desnovelamento
L-6	Célula muscular murina
M	Molar
NBT	Nitro-azul-tetrazólio

PBS	Tampão fosfato 50 mM, NaCl 0,15 M pH 7,2
Pro	Prolina
RNA	Ácido ribonucléico
RPMI	Meio Instituto Roswell Park Memorial
SDS-PAGE	Eletroforese em gel de poliacrilamida contando dodecil sulfato de sódio
Tris	Tris- hidroximetil-etano
Trp	Triptofano
U.I.	Unidade internacional
UV	Ultravioleta
v/v	Razão volume/volume
V_{max}	Velocidade máxima
ΔG	Energia livre de Gibbs

ÍNDICE

RESUMO

Esta tese descreve a identificação do gene *mtaf* (metiltioadenosina fosforilase) de *T. cruzi*, o qual contém uma fase aberta de leitura de 921 pb, sendo que sua a seqüência traduzida exibe a assinatura da família 2 das purina nucleosídeo fosforilase/MTAP. A seqüência da TcMTAF é 59% e 58% idêntica às seqüências MTAF do *Trypanosoma brucei* and *Leishmania major*, respectivamente, mas apresentando apenas 35% de identidade com a seqüência da MTAF humana. Além disso, o gene está representado como cópia única por genoma haplóide do parasita. A TcMTAF recombinante migra como um monômero de 33 kDa em gel de "SDS-PAGE" sob condições redutoras, mas se associa em oligômeros na ausência de agentes redutores. A MTAF nativa é expressa pelas três formas de desenvolvimento do *T. cruzi*. Apesar da enzima ser ativa em uma ampla faixa de pH e temperatura, ela exibe atividade máxima à 50 °C e um pH ótimo na faixa neutra. Ao contrário da MTAF humana, que degrada apenas MTA, a TcMTAF catalisa a clivagem de MTA, adenosina, deoxiadenosina e guanosina. Devido ao fato da TcMTAF e da MTAF humana possuírem diferentes parâmetros cinéticos e especificidade a substratos, a TcMTAF pode ser explorada como um novo alvo para o desenvolvimento de quimioterapia tripanocída. A rTcMTAP foi submetida a caracterização fisicoquímica. A enzima foi submetida à desnaturação térmica, visualizada por dicroísmo circular, em uma ampla faixa de pH, contudo não se observou uma relação entre a estabilidade da proteína e as condições de ionização do meio. A enzima demonstrou uma considerável resistência à desnaturação térmica, desdobrando-se em temperaturas acima de 79 °C. O conteúdo de estruturas secundárias da enzima é significativamente composto por α-hélices. Contudo, mesmo após a desnaturação térmica, a percentagem das α-hélices exibe pouca variação, principalmente no pH 7.4 e 9.0. Desnaturação química, induzida por hidrocloreto de guanidina e uréia, foi monitorada tanto por dicroísmo circular como por espectroscopia de fluorescência. A enzima suportou concentrações de até 3.6 M de hidrocloreto de guanidina e até 8 M de uréia sem alterar sua estrutura terciária. Os parâmetros termodinâmicos calculados a partir dos experimentos de desnaturação química e térmica demonstraram estar em harmonia. Em pH 6.0 e na presença de CTAB a enzima demonstrou uma resistência ainda maior à desnaturação térmica.

INTRODUÇÃO

INTRODUÇÃO

Doença de Chagas

A doença de Chagas, ou Tripanossomíase Americana, foi descoberta por Carlos Chagas, o qual identificou seu vetor, agente etiológico e descreveu suas características clínicas (Chagas, 1909). O mal de Chagas é prevalente no continente americano, representando a terceira maior endemia parasitária, atrás somente da Malária e da Esquistossomose (WHO, 1993). A doença é causada pelo parasita *Trypanosoma cruzi*, que infecta cerca de 21 milhões de pessoas (WHO, 2002), além de manter mais de 120 milhões indivíduos (25% da população da América Latina) sob risco de adquirir a infecção (WHO, 2002) .

Do ponto de vista econômico, a perda anual para o continente Latino Americano foi calculada em cerca de 6,5 bilhões de dólares (WHO, 1997); o Brasil gasta aproximadamente 750 milhões de dólares por ano no tratamento de pacientes chagásicos (WHO, 2000). Calcula-se que o investimento anual dos governos dos países latino-americanos, visando o controle da doença de Chagas, é muito inferior à perda econômica causada por esta endemia.

Vias de Transmissão

Existem várias vias de transmissão do T. cruzi, sendo que as principais são a vetorial ou via entomológica, a transfusional e a congênita, também chamada de transplacentária. Na via vetorial, a mais representativa, as formas infectantes do parasita presentes nas fezes dos triatomíneos entram em contato com a mucosa ou com a pele do indivíduo durante o repasto do inseto vetor (Prata, 2001). Há três ciclos de transmissão vetorial. O ciclo doméstico é o de maior importância epidemiológica, pois perpetua a infecção em seres humanos. No ciclo silvestre, os triatomíneos, uma vez contaminados, infectam roedores, marsupiais e outros animais silvestres. O terceiro ciclo é o peridoméstico, no qual intervêm mamíferos que, livremente, entram e saem das residências, atraindo os triatomíneos. Este ciclo serve de ligação entre os ciclos doméstico e silvestre (Brener *et alii*, 2000). Além desses, há relatos de transmissão via oral através de alimentos contaminados com o agente da doença.

Desenvolvimento da doença

As infecções causadas pelo T. cruzi podem ocorrer em três fases: aguda, latente ou indeterminada e crônica. A fase aguda é usualmente assintomática na maioria das pessoas infectadas e é caracterizada por febre, mialgia e mal-estar (Deghaide *et alii*, 1998). Em alguns pacientes, o sinal de Romaña (inchaço unilateral, bipalpebral) e o chagoma de inoculação são sinais indicativos da porta de entrada do parasita no hospedeiro humano(Brener *et alii*, 2000). Miocardites e meningoencefalites podem ocorrer ocasionalmente (Deghaide *et alii*, 1998). Estima-se que metade dos indivíduos infectados pelo T. cruzi entram na fase latente, (Macedo, 1980) na qual não apresentam as alterações patológicas típicas da doença. Após 20 anos de fase indeterminada, aproximadamente 30% dos indivíduos infectados desenvolvem a fase crônica (ElMunzer *et alii*, 2004). As manifestações clínicas mais freqüentes são as cardiopatias, disritmias, tromboembolismo e infarto do miocárdio, sendo que alterações no trato digestivo (megaesôfago e megacólon) e no sistema nervoso também podem ocorrer (Prata, 2001).

O protozoário flagelado apresenta três formas de desenvolvimento durante o seu ciclo de vida que foram classificadas em função da sua morfologia e biologia (Brener, 1972). As formas são: epimastigota, forma replicativa, presente no intestino médio do vetor; tripomastigota, forma infectante do parasita encontrada no hospedeiro vertebrado, também chamada de tripomastigota metacíclica; amastigota, a forma intracelular replicativa do hospedeiro mamífero (Tanowitz *et alii*, 1992).

Ciclo de Vida do *Trypanosoma cruzi*

O ciclo evolutivo do *T. cruzi* no hospedeiro vertebrado inicia-se quando as formas tripomastigotas metacíclicas são eliminadas nas fezes e urina do inseto, durante seu repasto sangüíneo, penetrando na mucosa do hospedeiro. Nas células do hospedeiro, as tripomastigotas convertem-se em amastigotas replicativas que residem no citoplasma da célula do hospedeiro. Independente da via de infecção, amastigotas intracelulares, após sucessivas divisões binárias, transformam-se em tripomastigotas flageladas que, após romper a célula do hospedeiro, circulam na corrente sangüínea. As formas tripomastigotas podem invadir qualquer tipo celular, propagando a infecção pelo corpo (Brener *et alii*, 2000). Por fim, os tripomastigotas adquiridos durante a alimentação do triatomíneo com o sangue contaminado transformam-se em epimastigotas no trato digestivo do inseto antes de diferenciarem-se em formas tripomastigotas metacíclicas infectantes (Figura 1) completando o ciclo.

Figura 1. Esquema do ciclo de vida do *Trypanosona cruzi* e seus principais hospedeiros (TDR/Welcome Trust).

Purina nucleosídeo fosforilase.

As enzimas da família Purina nucleosídeo fosforilase, do inglês "purine nucleoside phosphorylase" (PNP, E.C. 2.4.2.1) catalisam a quebra da ligação glicosídica de ribo e deoxiribonucleosídeos gerando base purínica e ribose (deoxiribose)-1-fosfato, na presença de fosfato inorgânico (Pi), seu segundo substrato. Esta reação é direcionada, termodinamicamente, em favor da síntese de nucleosídeo (Friedkin, 1950). Contudo, nas células a fosforólise é altamente favorecida em detrimento da síntese, devido ao acoplamento com reações enzimáticas subsequentes. PNP é uma enzima ubíqua do metabolismo de purina, desempenhando papel na via de salvação dessa base, incluindo aquelas de parasitas protozoários, o que permite as células utilizarem as bases purínicas recicladas para síntese de nucleotídeos purínicos (Bzowska *et alii*, 2000).

A ubiqüidade das PNPs e sua distribuição em diversos tecidos e células foi documentado no passado por (Agarwal *et alii*, 1972; Stoeckler, 1984). Em humanos, a atividade mais intensa foi encontrada no rim, linfócitos periféricos e granulócitos. Contudo, levado em conta o volume celular, as células vermelhas mostram o mesmo nível de atividade que linfócitos periféricos. Logo, eritrócitos humanos, deficientes na síntese *de novo* de purinas e consequentemente dependente da reciclagem da mesma, são a maior fonte de PNP. Entretanto, eritrócitos de camundongos, ratos e outros animais contêm níveis de PNP consideravelmente menores, um fator importante na hora de extrapolar resultados de animais de laboratório para humanos (Stoeckler, 1984).

Além da fosforólise de nucleosídeos oriundos da degradação do DNA, as PNPs também atuam como enzima de salvação de substratos purínicos requeridos pela hipoxantina-guanina fosforibosiltransferase (HGFRT) para sintetizar os monofosfatos de inosina e guanosina, que serão por fim convertidos a deoxi-ribonucleotídeos pela enzima ribonucleotídeo redutase (Bzowska *et alii*, 2000).

A deficiência de PNP foi descrita pela primeira vez em 1975 (Giblett *et alii*, 1975), sendo uma condição rara, associada com uma forma de imunodeficiência celular, não humoral, recessiva autossômica. Os genótipos mutantes de PNPs responsáveis por esta condição tem sido identificada em inúmeros pacientes (Markert *et alii*, 1997). Estão incluídos nessas mutações, troca de padrão de leitura da ORF (frameshift) assim como erro na direção da tradução (missense), contudo a mais comum é a mutação pontual Arg234Pro. Baseado na estrutura tridimensional da PNP de eritrócito humano foi mostrado que as principais mutações afetam o sítio ativo da enzima (Erion *et alii*, 1997).

As apresentações clínicas da deficiência homozigótica de PNPs em humanos incluem infecções recorrentes e linfopenia severa nos 2 primeiros anos de vida. Populações e funções de células T ficam reduzidas, enquanto as funções das células B são preservadas. Anemia hemolítica autoimune e neutropenia, lupus eritrematoso sistêmico, e linfomas de células B são observados nesses pacientes. Anormalidades neurológicas foram reportadas em mais de 50% das crianças afetadas pela deficiência de PNPs (Gilbertsen *et alii*, 1990; Hershfield *et alii*, 1995).

Acredita-se que as alterações em células T deficientes em PNP está relacionada com o acúmulo de dGTP que causa inibição da ribonucleotídeo redutase via retroalimentação negativa, bloqueando a redução da citidina di-fosfato (CDP) em deoxi-CDP (dCDP), necessária para a síntese de DNA, o que impede a maturação e diferenciação das células T. Contudo, em células B, não ocorre o acúmulo de dGTP pois estas apresentam atividade de diversas nucleotidases (Hershfield *et alii*, 1995). Contudo, mecanismos adicionais para o efeito do acúmulo de dGTP sobre as células T foram sugeridos (Duan *et alii*, 1990), onde a inibição da ribonucleotídeo redutase é um evento acessório, e outros mecanismos podem estar operando, como a inibição da síntese de RNA. Inclusive estudos com inibidores específicos para PNP apontam para a inibição de uma enzima que participa da síntese de DNA, mas que seja improvável ser a ribonucleotídeo redutase, pois o efeito dos inibidores não foi aumentado com a adição de dGTP.

Além disso, as PNPs têm a capacidade de realizar a reação oposta, síntese de nucleosídeos. Esta característica, apesar de menos estudada, é explorada para fins biotecnológicos, servindo de ferramenta para produção de análogos de nucleosídeos com potencial antiviral (Burns *et alii*, 1993) e anti-neoplásico (Chae *et alii*, 1998). A descrição dessa aplicação dessas enzimas foi documentado por Krenitsky et al (Krenitsky *et alii*, 1981). Outra aplicação relatada é utilização em sensores microeletrônicos, onde a partir da associação de enzimas foi possível detectar liberação de purina ou fosfato *in vitro* e *in vivo* (Haemmerli *et alii*, 1990; Llaudet *et alii*, 2003).

Classificação:

PNPs com diferentes especificidade já foram identificadas em uma ampla gama de organismos. Com base em vários critérios foram sugeridas algumas classificações.

Uma delas baseia-se na especificidade a substratos e número de subunidades por oligômero, e foi dividida em duas categorias principais:

(1) Homotrímeros de baixa massa molecular, peso molecular (M_r) ~ 80 - 100 kDa, especificidade para 6-oxopurinas e seus nucleosídeos. Essa categoria também é chamada de "Ino-Guo fosforilases", e listadas no banco de dados SWISS-PROT como "Fosforilases família 2 - PNP/5'-deoxi-5'-metiltioadenosine fosforilase (MTAF) (Pugmire *et alii*, 2002). Enzimas desse tipo foram isoladas de diversos tecidos de mamíferos (Agarwal *et alii*, 1972; Stoeckler, 1984) e também de microorganismos como *Bacillus stearothermophilus* (Hamamoto *et alii*, 1996), *Cellulomonas* sp. (Bzowska *et alii*, 1998).

(2) Homohexâmeros de alta massa molecular, M_r ~ 110 – 160 kDa, ampla especificidade, aceitando tanto 6-oxo e/ou 6-aminopurinas e seus nucleosídeos. No banco de dados SWISS-PROT recebem a denominação de "Fosforilases família 1 – PNP/UDP". Enzimas dessa categoria foram identificadas principalmente em microorganismos como *Salmonella typhimurium* (Jensen *et alii*, 1975), *Klebsiella sp.* (Takehara *et alii*, 1995) and *Sulfolobus solfataricus* (Cacciapuoti *et alii*, 1994).

Contudo essa é uma tentativa de classificação que se baseia nas características supracitadas e nas propriedades das quatro enzimas, de organismos diferentes, que tiveram suas estruturas tridimensionais resolvidas e depositadas no *Protein Data Bank* (PDB). (Ealick *et alii*, 1990; Mao *et alii*, 1997; Bzowska *et alii*, 1998). Essas enzimas foram isoladas de eritrócitos humanos (PDB 1ULA), baço bovino (1VFN), *Cellulomonas* sp (PDB 1QE5) e *Escherichia coli* (PDB 1ECP).

Como em toda tentativa de classificação existem enzimas de diversos organismos que apresentam características de ambas as famílias. Por exemplo, uma das duas PNPs codificadas pelo *B. stearothermophilus* (Hori *et alii*, 1989b) apresenta especificidade e massa da subunidade similar às Ino-Guo mas a filtração em gel indica que ela forma um dímero. Já a outra PNP tem especificidade das enzimas hexaméricas, mas adota configuração de tetrâmero em solução (Hori *et alii*, 1989a). Ainda mais aberrante é a PNPII de *E. coli*, isolada de mutantes *xapR* (Buxton *et alii*, 1980) que aceita xantosina, mas diferente de outras enzimas de baixa massa molecular, também aceita adenosina e deoxi-adesonia como substratos. Essas enzimas que não se encaixam

perfeitamente nas características gerais descritas ficam agrupadas em um terceiro grupo, onde as enzimas podem apresentar especificidade das PNPs de baixa massa mas não são homotrímeros ou apresentar especificidade das de alta massa molecular e não são homohexâmeros. Alguns exemplares desse grupo foram identificadas em bactérias (e.g., *Proteus vulgaris*), mamíferos (e.g., mitocôndria hepática bovina) e parasitas (e.g., *Plasmodium falciparum*) (Bzowska *et alii*, 2000).

Subfamília MTAF

Dentre os membros da família PNP, a enzima MTAF (E.C. 2.4.2.28) tem sido amplamente estudada, tanto a de origem humana quanto a de parasitas e microorganismos. Como esperado, esta enzima catalisa a clivagem nucleosídeos pelo intermédio de fosfato, contudo sua especificidade está voltada para o nucleosídeo modificado metiltioadenosina (MTA), porém com capacidade de metabolizar outros nucleosídeos purínicos.

MTAF humana

A MTAF humana, abundantemente encontrada em todas as células normais incluindo eritrócitos e células da medula óssea, é ausente em diversos tipos de cânceres como gliomas, câncer de pulmão de células não-pequenas, leucemia não-linfóide aguda, e melanoma (Della Ragione *et alii*, 1996; Schmid *et alii*, 1998; Behrmann *et alii*, 2003). O gene *mtap* está localizado no cromossomo 9p21 a uma distancia de 100 Kb dos genes supressores de tumor *p16* e *p14*, igualmente ausentes em diversos tipos de tumor (Della Ragione *et alii*, 1996). Uma primeira hipótese para explicar a ausência de atividade da MTAF em tumores era a co-remoção homozigótica do gene *mtaf* com os genes supressores de tumor devido apenas a distância entre eles. Contudo, dados mais recentes sugerem que MTAF por si pode funcionar como um supressor de tumor. Por exemplo, demonstraram a ausência de MTAF não concomitante com a perda de *p16* tanto em câncer de pulmão de células-não-pequenas como em gliomas (Schmid *et alii*, 1998; Brat *et alii*, 1999). Além disso, a re-expressão de MTAF em células de adenocarcinoma de mama extinguem o crescimento *in vitro* e inibe a formação de tumor em camundongos imuno-deficientes (Christopher *et alii*, 2002). Um último dado mostra que a expressão de MTAF em células Mel Im de melanoma humano resulta em uma redução substancial do potencial invasivo dessas células (Behrmann *et alii*, 2003). Uma possível explicação para o efeito supressor de tumor é a influência da MTAF sobre a produção de poliaminas. A ausência da enzima causa ativação extra da enzima ornitina descarboxilase (ODC), passo limitante da produção de poliaminas nas células humanas

(Subhi *et alii*, 2003). Inclusive demonstrou-se que a sua super-expressão maligniza fibroblastos *in vitro* como também aumenta a freqüência de tumores de pele em camundongos transgênicos (Moshier *et alii*, 1993; O'Brien *et alii*, 1997). A partir da deficiência encontrada nesses diversos tipos de tumores vislumbrou-se a oportunidade de desenvolver uma terapia seletiva que pouparia as células normais. Esta parte do pressuposto que células deficientes em MTAF têm maior dependência da síntese *de novo* de nucleotídeos de adenina. A utilização bloqueadores da síntese *de novo* mataria as células MTAF-deficientes e as células normais seriam poupadas devido à reciclagem do MTA pela MTAF, suprindo adenina dessa forma (Batova *et alii*, 1999).

MTAF de parasitas

Esta enzima está presente em diversos parasitas como *Trypanosoma cruzi* (Miller *et alii*, 1987), *Trypanosoma brucei* (Ghoda *et alii*, 1988), *Schistosoma mansoni* (Savarese *et alii*, 1989), *Leishmania donovani* (Koszalka *et alii*, 1986) e é considerada um promissor alvo de drogas. Isto se deve principalmente porque a MTAF de parasitas, apesar de apresentar similaridades com a enzima de mamíferos, tem importantes diferenças. A enzima dos parasitas demonstra uma elevada especificidade em relação a outros nucleosídeos como adenosina e seus análogos (Ghoda *et alii*, 1988), o que não ocorre com a enzima de mamíferos. Tal fato auxilia o desenvolvimento de substratos subversivos seletivos apenas contra a enzima dos patógenos. Outra importante diferença, relacionada apenas aos tripanossomatídeos, é que estes não apresentam a síntese *de novo* de purinas. Fato que reforça esta via como alvo devido à grande dependência por fontes exógenas desses nucleosídeos, principalmente de adenina (Fish *et alii*, 1982) . O uso de análogos tóxicos já se mostrou efetivo contra *T. brucei*, inclusive acarretando a cura de infecções em camundongos (Bacchi *et alii*, 1997). Além disso, acredita-se que a inibição da síntese de poliaminas, que é a fonte de produção do MTA, irá intensificar o uso de substratos tóxicos pelos parasitas. Inclusive já foi demonstrado que tripanosomas africanos são bastante sensíveis à inibição da biosíntese dessas moléculas (Bacchi *et alii*, 1983; Bacchi *et alii*, 1987). Tais fatos levam a assumir que associando o uso de inibidores de poliaminas com substratos tóxicos da MTAF resultará em efeito sinérgico contra os tripanossomatídeos, suposição não testada até a presente data.

Via metabólica do MTA

Poliaminas são cátions presentes em praticamente todas as células. As mais comuns são putrescina, espermidina e espermina. Pelo fato de serem cátions em pH fisiológico, por apresentarem conformação flexível e se ligarem reversivelmente a moléculas carregadas negativamente, as poliaminas desempenham uma variada gama de papéis bioquímicos, incluindo: cofator para síntese de macromoléculas, divisão e diferenciação celular e também como estabilizador conformacional de ácidos nucléicos (Cohen, 1998). Basicamente a produção delas se dá pela adição de grupos aminopropil transferidos da *S*-adenosilmetionina descarboxilada (dAdomet) para putrescina e espermidina, pelas enzimas espermidina e espermina sintase, respectivamente. Como subproduto dessa reação ocorre a formação do nucleosídeo metiltioadenosina (MTA). O MTA também é produzido na via da homoserina lactona, contudo sua contribuição para o total produzido não é conhecida, conferindo à via das poliamias a maior fonte desse metabólito (Williams-Ashman *et alii*, 1982; Walker *et alii*, 1997).

A existência do nucleosídeo metiltioadenosina (5'-deoxi-5'-metiltioadenosina), comummente abreviado a MTA, foi descoberta há quase um século (Williams-Ashman *et alii*, 1982). Sua estrutura molecular foi descrita em 1924 e sua importância metabólica ficou aparente em 1952, em estudos sobre a relação entre metionina e 5'-tiometilribose. Devido à sua concomitância com a produção de poliaminas, o MTA está presente em todos os tipos de organismos, incluindo procariotos, protozoários, levedura, plantas e eucariontes (Williams-Ashman *et alii*, 1982).

O MTA é um nucleosídeo de adenina, hidrofóbico e que contém enxofre, no qual a sua ribose teve a hidroxila da posição 5' substituída por um motivo metiltio. Este motivo é derivado do aminoácido metionina, enquanto o resto da molécula vem do ATP.

O MTA está localizado numa encruzilhada do metabolismo celular, fazendo parte das vias de produção de poliaminas, salvação de purinas e de metionina. A Figura 2 representa um esquema das vias metabólicas às quais o nucleosídeo está integrado. O MTA é rapidamente clivado pela MTAF em adenina e metiltioribose-1-fosfato (MTR1P). A adenina é regenerada a adenosina e posteriormente a AMP em mamíferos ou no caso de vários parasitas diretamente a AMP pela enzima fosforibosiltransferase (el Kouni, 2003). Já o MTR1P é regenerado a metionina através de uma cascata enzimática.

Purinas são de vital importância para todos os organismos. Elas são essenciais para a síntese de ácidos nucléicos, proteínas e outros metabólicos, como também reações que requerem energia. Já a metionina, além do papel indispensável na formação proteínas, também é o metabólito precursor da Adomet, que está diretamente ligada à síntese de poliaminas, e ao processo de metilação de proteínas, lipídios e DNA.

Devido ao fato do MTA estar relacionado à via de salvação de dois precursores metabólicos de ávido consumo em células que se replicam constantemente, por exemplo *Trypanosoma cruzi*, *Trypanosoma brucei brucei*, *Giadia lamblia*, *P. falciparum*, entre outros, e por existirem diferenças entre humanos e parasitas, a via de reciclagem do MTA constitui um interessante alvo para desenvolvimento de novas drogas contra parasitas (Walker *et alii*, 1997; el Kouni, 2003).

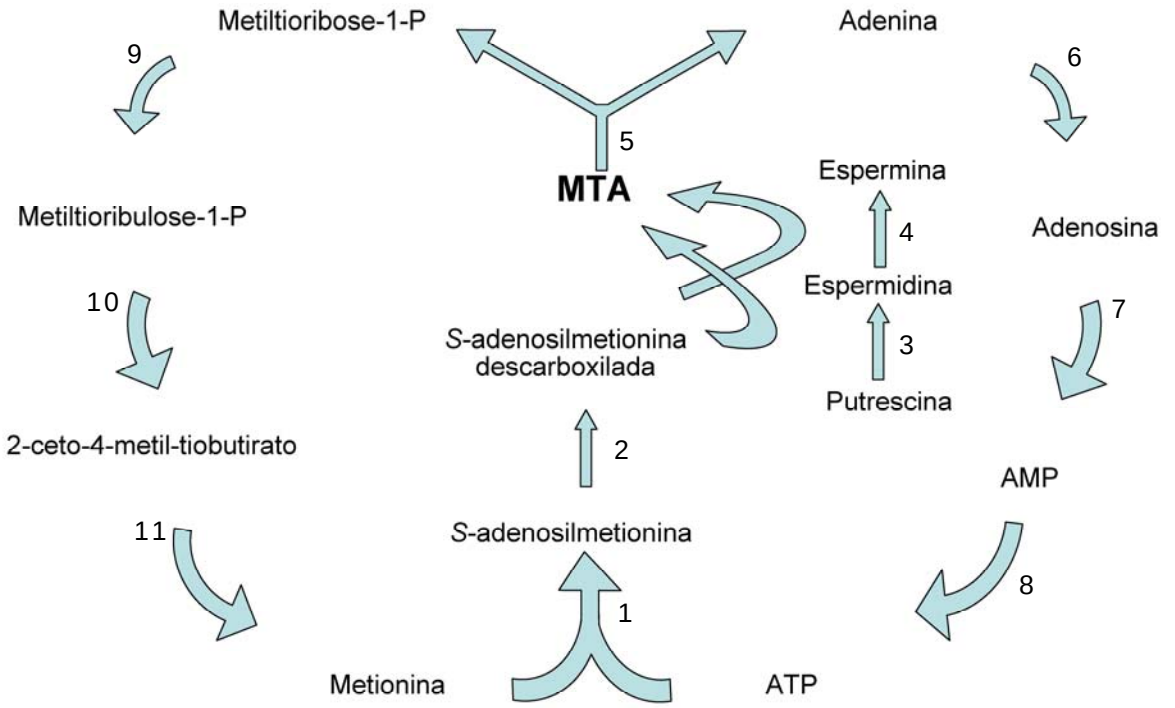

Figura 2. Via metabólica de síntese e metabolismo do nucleosídeo 5'-metiltioadenosina. O precursor do MTA, Adomet, é sintetizado pela enzima metionina adenosiltransferase (1). Em seguida, Adomet é descarboxilado pela Adomet descarboxilase (2). Adomet descarboxilada então é utilizada na síntese de poliaminas. Espermidina sintase (3) e espermina sintase (4) transferem o grupo propilamina da Adomet descarboxilada para putrescina e espermidina, respectivamente, em duas reações seqüenciais. A partir dessas duas reações ocorre a produção de MTA, substrato para a metiltioadenosina fosforilase (5). A última então catalisa a primeira reação de reciclagem de adenina e de metionina. Adenina é convertida a em ATP pela ação das enzimas Ade-fosforibosiltransferase (6) seguida da adenosina quinase (7) e finalmente fosforilado a ATP (8). A partir do outro produto da ação da MTAP, metiltioribose-1-P, o isômero metiltioribulose-1-P é gerado pela aldose-cetose isomerase (9). Este metabólito então sofre uma série de oxidações (10) resultando no 2-ceto-4-metil-tiobutirato, que é finalmente transaminado a metionina por uma aminotransferase (11).

Princípios teóricos da caracterização termodinâmica

Dicroísmo circular (CD do inglês *circular dichroism*) é a técnica espectroscópica relacionada à absorção diferenciada dos componentes circularmente polarizados para esquerda e direita de uma radiação plano-polarizada. Este efeito ocorre quando um cromóforo é quiral (opticamente ativo) pelo fato: (a) de ser intrínseco a sua estrutura, ou (b) estar covalentemente ligado a um centro quiral ou (c) estar situado em um ambiente assimétrico. Após os componentes da radiação eletromagnética passarem pela amostra e sendo um deles absorvido em maior amplitude, a radiação resultante estará elipticamente polarizada, isto é, a resultante terá uma trajetória em forma de elipse.

As propriedades biológicas de uma proteína estão intimamente relacionadas à sua estrutura tridimensional, as quais podem ser influenciadas por fatores químicos e físicos como, temperatura, pH e ligantes. Apesar do número elevado de estruturas atômicas de proteínas depositadas no bando de dados PDB pouco se sabe sobre o processo de dobramento destas moléculas. Decifrar o mecanismo responsável pelo dobramento correto e assim estabelecer a relação entre seqüência e estrutura tridimensional é de grande interesse biológico como também representaria grande avanço tecnológico e médico. A relevância clínica pode ser ilustrada pelo fato de que certas doenças são causadas pelo dobramento incorreto de proteínas, como a fibrose cística (Sifers, 1995; Thomas *et alii*, 1995). Informações sobre as etapas de dobramento protéico foram adquiridas principalmente a partir de polipeptídios pequenos, inclusive com a definição de características estruturais de fases intermediárias e da cinética de processos-chave, sendo que o DC desempenhou importante papel na obtenção desses dados.

Dicroísmo Circular e desnaturação térmica

A técnica de DC permite analisar várias características estruturais de proteínas. Estudos na região do ultravioleta (UV)-distante (de 240 a 180 nm) permitem quantificar o conteúdo total de estruturas secundárias da proteína. Nessa faixa de comprimento de onda, a radiação eletromagnética é absorvida principalmente pelas ligações peptídicas. Já se sabe há vários anos que as formas regulares de estrutura secundária exibem perfis distintos no espectro de CD com UV-distante. A dedução do conteúdo de cada estrutura secundária na proteína pode ser estimada por comparação do espectro com um conjunto de espectros de proteínas que já tem sua estrutura tridimensional resolvida por

cristalografia de raios-X (Provencher *et alii*, 1981). Outra utilidade decorrente é acompanhar as modificações da proteína durante processo de desdobramento por calor ou por agentes denaturantes. Essas modificações também podem ser acompanhadas por outros métodos espectroscópicos como emissão de fluorescência dos resíduos aromáticos da proteína, este tópico será posteriormente analisado.

Com a obtenção de espectros em temperatura crescente pode-se analisar o efeito desta sobre a molécula e determinar a região da transição entre estado nativo e desnaturado. A curva de desdobramento analisada matematicamente permite calcular os parâmetros que caracterizam a estabilidade de proteínas. Previamente, é importante estabelecer se a molécula em questão desnatura em um modelo de dois estados (isto é, nativo e desdobrado) ou outro mais complexo. Isto pode ser observado (a) pelo formato da curva de transição entre os estados e/ou (b) coincidência das curvas de transição monitoradas por diferentes métodos espectrofotométricos e/ou (c) equivalência do ΔH calculado experimentalmente por microcalorimetria com o obtido do gráfico de van't Hoff. Em modelo de dois estados é possível calcular diretamente a variação na energia livre (ΔG) do processo de desdobramento. Este parâmetro é obtido a partir da extrapolação da faixa de transição até a temperatura de 25 °C (estabilidade térmica) ou de ausência de desnaturante (estabilidade química). O uso de extrapolação linear normalmente gera valores de ΔG e dos outros parâmetros que estão em concordância com os derivados de estudos calorimétricos (Teles *et alii*, 2005), contudo o contrário pode acontecer devido a processos de desnaturação mais complexos, aos quais o CD é menos sensível (Tello-Solis *et alii*, 1995). Os parâmetros termodinâmicos provêm dados para comparação de estabilidade entre proteínas diferentes, ou mutantes de uma mesma, como também permite quantificar o efeito de modificações no microambiente sobre uma única proteína. Um exemplo é a proteína deidroquinase de *Salmonella typhi*, a qual a partir da alteração de um derivado imina de uma única lisina tem sua estabilidade química e térmica aumentada em quase 100%, de 1,6 para 4,5 M de hidrocloreto de guanidina e de 56 para 98 °C, respectivamente. Estudos de CD usando UV-distante e próximo revelaram que esse aumento na estabilidade não envolve nenhuma modificação substancial na estrutura secundária e terciária da proteína (Moore *et alii*, 1993).

Espectroscopia de Fluorescência

A espectroscopia de fluorescência, com suas múltiplas aplicações para análise de proteínas e para ciências da vida em geral, passou por rápido desenvolvimento na última década. Quando uma molécula absorve radiação visível e UV ela passa para o estado de excitação eletrônica ou eletrônica e vibracional simultaneamente. Uma parte da energia absorvida é transferida para outros níveis energéticos como os níveis vibracionais, fônons, energia térmica, entre outros. A energia remanescente é emitida como fótons com comprimento de onda maior do que o absorvido. Inclusive, algumas reações químicas têm a característica de emitir radiação enquanto estão ocorrendo. Em termos gerais, a radiação emitida nesses processos é chamada luminescência. Métodos de análise muito sensíveis utilizam fenômenos específicos da luminescência como a fluorescência, fosforescência e quimiluminescência.

As transições no nível eletrônico e vibracional envolvidas no fenômeno da luminescência podem ser entendidas com a ajuda do diagrama de energia de Jablonski (Figura 2). Um estado eletrônico excitado (S_1 ou S_2) é observado quando um elétron, localizado na orbital molecular ocupada de mais alta energia de um estado eletrônico fundamental (S_0), passa para a próxima orbital de maior energia desocupada. A excitação geralmente é acompanhada por mudanças no estado vibracional da molécula. Primeiramente ocorre a relaxação do estado excitado para um nível vibracional mais baixo, que ocorre por meio de uma transição não radioativa. Esta é seguida pela fluorescência, que é a relaxação para o estado eletrônico fundamental por meio da emissão de radiação eletromagnética.

O triptofano absorve radiação devido às transições de energia ocorridas no seu anel indol. Em solução aquosa o aminoácido triptofano exibe espectro de fluorescência máximo em 350 nm. A excitação do anel indol leva ao aumento substancial do momento dipolo, acarretando em deslocamentos de emissão mais intensos. Este deslocamento é causado pelos processos de relaxação orientada, envolvendo o dipolo do cromóforo e do solvente.

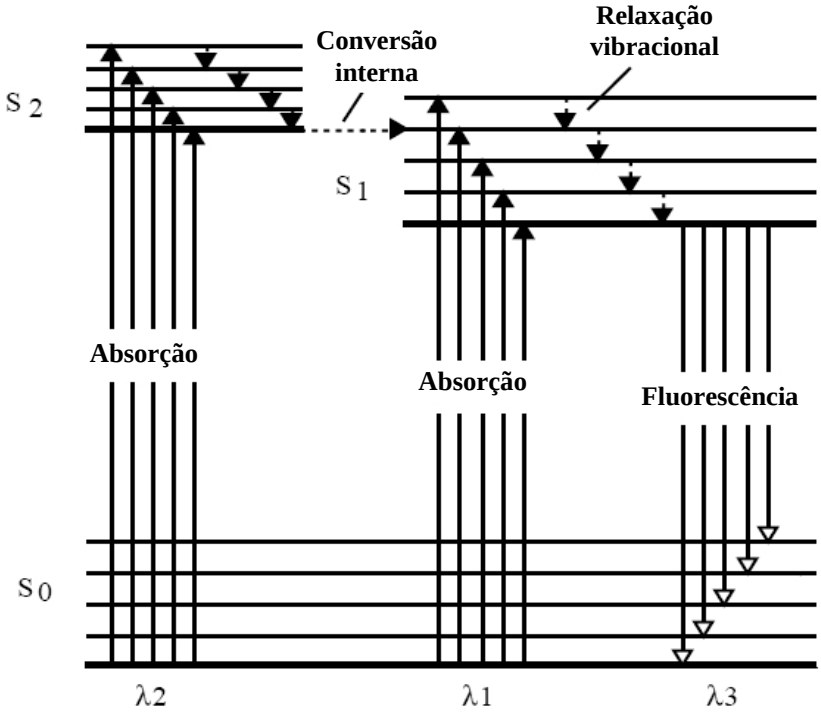

Figura 2. Diagrama de Jablonski, parcialmente representado, mostrando os processos que levam a luminescência.

A sensibilidade do triptofano à polaridade e mobilidade do ambiente faz de sua fluorescência uma importante ferramenta em estudos de dinâmica e estrutura de proteína. A fluorescência do triptofano sofre atenuação (*quenching*) pela água e que leva frequentemente a um decréscimo no rendimento quântico em situações de desnaturação da proteína, momento em que o triptofano se encontra exposto a um ambiente aquoso. Contudo existem exceções a essa regra, que causa a atenuação da emissão do triptofano mesmo com a proteína em seu estado nativo, por exemplo, ligações dissulfeto, os aminoácidos lisina e arginina quando estão carregados, histidina quando se encontra protonada, absorção por grupo heme, entre outros (Burstein, 1976; Burstein, 1977; Colucci *et alii*, 1990). A atenuação também pode ser causado por uma variedade de substâncias entre elas, oxigênio, iodeto, acrilamida, Cs^{2+}, Cu^{2+}. Além disso, a partir da atenuação causada por esses reagentes causam é possível mensurar o quão acessível está um resíduo de triptofano de uma proteína.

Além do triptofano, moléculas biológicas contêm outros fluoróforos naturais. O triptofano é o aminoácido que apresenta maior fluorescência em proteínas e por isso é dado como o responsável pela fluorescência dessas biomoléculas. O aminoácido que emite a segunda maior fluorescência é a tirosina, contudo a sua aplicação está limitada a

proteínas que não contém triptofanos em sua seqüência. Estudos que utilizam a fluorescência da fenilalanina como parâmetro são raros devido ao seu fraco rendimento quântico.

A espectroscopia de fluorescência é fundamental no estudo do dobramento de proteínas (Eftink, 1994; Eftink *et alii*, 1997). Por exemplo, a fluorescência intrínseca, juntamente com outros métodos, foi utilizada para corroborar a transição em dois estados do inibidor de quimiotripsina (Jackson *et alii*, 1991). A observação da fluorescência é usada para acompanhar a desnaturação ou renaturação de proteínas sob influência de mudanças na temperatura, pH ou adição de solutos, por exemplo, denaturantes. O desdobramento das proteínas resulta num aumento da exposição do triptofano ao ambiente aquoso revelado pelo deslocamento da fluorescência em direção a comprimentos de onda na faixa do vermelho (efeito batocrômico). Outros parâmetros determinados a partir da fluorescência, como intensidade, distribuição temporal, constante de Stern-Volmer, eficiência de transferência de energia não-radiotiva podem ser utilizados em estudos de dobramento de proteína.

OBJETIVOS

OBJETIVOS

OBJETIVO GERAL:

O objetivo geral do nosso trabalho é melhor entender a fisiologia do parasita *T. cruzi* e identificar diferenças entre as suas vias metabólicas e as do hospedeiro mamífero permitindo determinar novos alvos de drogas. Neste contexto, a caracterização molecular e biofísica da TcMTAP mostrou-se interessante devido à grande dependência do parasita pelas vias associadas a esta enzima. Acreditamos que essa fosforilase desempenha papel importante na manutenção da vida do *T. cruzi* e que apresenta diferenças moleculares suficientes para torna-la um promissor objeto de estudo vislumbrando o desenvolvimento de quimioterápicos mais específicos para o tratamento da doença de Chagas. Nossa pesquisa tem como objetivos específicos:

- Determinar a quantidade de cópias do gene *mtaf* presentes no genoma do *T. cruzi*.
- Caracterizar as propriedades cinéticas da enzima MTAF recombinante.
- Determinar o padrão de expressão da MTAF nativa nas diferentes formas do parasita.
- Caracterizar a estabilidade estrutural da MTAF recombinante.
- Determinar a especificidade da enzima a substratos.

RESULTADOS

Os resultados deste estudo estão apresentados na forma de manuscritos a serem submetidos à publicação em periódicos internacionais indexados. Os manuscritos são:

1. **"The methylthioadenosine phosphorylase of *Trypanosoma cruzi* is mesophilic and displays broad substrate specificity."**
2. **"The drug target methylthioadenosine phosphorylase of *Trypanosoma cruzi* exhibits remarkable resistance to thermal and chemical denaturation."**

THE METHYLTHIOADENOSINE PHOSPHORYLASE of *Trypanosoma cruzi* IS MESOPHILIC AND DISPLAYS BROAD SUBSTRATE SPECIFICITY

David Neves, Izabela Dourado Bastos, Meire Maria de Lima, Gloria Restrepo-Cadavid, Antonio R. L. Teixeira, Francisco Javier Medrano, Philippe Grellier, Joseph Schrével, David Engman and Jaime Martins Santana.

Summary

Methylthioadenosine phosphorylase (MTAP) is an enzyme found in all eukaryotes and plays major role in the purine and methionine salvage pathways. Trypanosomatids, single-celled eukaryotes, are unable to synthesize purine rings de novo and thus are dependent on the purine salvage pathway. For this reason, the purine salvage pathway is a potential target for the treatment of diseases caused by trypanosomatids. In this study, we present the characterization of the MTAP of the trypanosomatid *Trypanosoma cruzi* (TcMTAP). *T. cruzi* is the aetiological agent of Chagas disease, an incurable sickness responsible for thousands of deaths in Latin America. The TcMTAP gene contains an open reading frame of 921 bp, whose translated sequence shows the purine nucleoside phophorylase/MTAP family 2 signature. The TcMTAP sequence is 59% and 58% identical with MTAP sequences of *Trypanosoma brucei* and *Leishmania major*, respectively, but only 35% identical with the sequence of human MTAP. Recombinant TcMTAP migrates as a 33 kDa monomer by SDS-PAGE under reducing conditions, but assembles into oligomers in the absence of reducing agents. Native MTAP is expressed by the different developmental stages of *T. cruzi*. Although the enzyme is active in a broad range of pH and temperature, it has a neutral pH optimum and displays maximal activity at 50°C. In contrast to human MTAP, which cleaves only MTA, TcMTAP mediates cleavage of MTA, adenosine, deoxyadenosine and guanosine. Because TcMTAP and human MTAP possess different kinetic parameters and substrate specificities, TcMTAP could be exploited as a novel target for the development of trypanocidal chemotherapy.

Introduction

Chagas' disease is an illness caused by the trypanosomatid protozoan *Trypanosoma cruzi* and afflicts more than 18 million people in the American continent, from the south of Argentina to the south of the USA [1]. The disease is known over 90 years but a total curative drug is not available yet. The drugs currently used to treat *T. cruzi* infections often present low specificity and considerable toxicity, therefore newer compounds are being tested [2]. In lack of an efficient treatment for Chagas disease, there is an urge to define metabolic targets for the development of new drugs to treat and control consumptive chronic disease. The existing evolutionary differences between parasitic and human enzymes allow rational drug design, aiming at the development of new and specific compounds for the chemotherapy of "so called" incurable diseases [3,4]. For example, the pathogenic trypanosome´s purine transport system, which is absent in mammalian cells, allows the use of subversive analogs [5-7]. It has been shown that the purine and polyamine metabolism are essential to the trypanosomatids' life and, thus, promising pathways for such approach [8]. Purines serve as precursor molecules for DNA and RNA, as carriers of high-energy phosphate bonds, as constituents of coenzymes and as modulators of certain enzymes. Methionine besides a constituent of proteins also has a key participation in protein methylation and polyamine biosynthesis. For instance, *Trypanosoma brucei* intensively uses methionine to methylate proteins and lipids and to form polyamines that play crucial roles in replication, differentiation and cellular growth. [9-11].

The methylthioadenosine phosphorylase [12] is a key enzyme associated with both purine and methionine salvage pathways. MTAP cleaves the sulfur-containing nucleoside MTA, a byproduct of the polyamine production, to adenine and methylthioribose-1-phosphate (MTR1P). The adenine will replenish the purine pool and

MTR1P is converted again to methionine in a five-step enzyme reaction [13]. The amount of recycled methionine plays an important role in polyamine production [4]. The purine salvage pathway, part of the purine metabolism, becomes even more important in trypanosomatids because they lack the molecular machinery to the *de novo* synthesis of the purinic ring [14,15]. Therefore, uptake and salvage pathways are the main sources of purines for these protozoans [16,17]. Purine metabolism in pathogenic protozoans appears to offer several opportunities for chemotherapy: a) because no *de novo* synthesis of these compounds occurs, interdiction of the salvage pathway has far greater implications than interruption of similar pathways in mammals; b) some of the enzyme systems are capable of accepting purine analogs and metabolizing them to nucleotides; c) these analogs serve as metabolic inhibitors [18,19].

MTAPs (E.C. 2.4.2.28) belong to the purine nucleoside phosphorylase (PNP) family. It has been proposed that this family should be divided into low- and high-molecular mass categories based on primary sequence homology, quartenary structure and substrate specificity. Whereas PNP proteins do not usually show high sequence homology, structure comparisons show striking significant similarities [20,21]. The members of this family are ubiquitously distributed in nature, from Archaea to human, showing heterogeneous kinetics and substrate preferences [20].

MTAPs of protozoan parasites have been categorized as potential chemotherapeutic targets because of their relation to crucial physiological processes, purine and methionine salvage and the important differences between the host and the parasite metabolism in these pathways. [10,22,23]. The African trypanosome *T. brucei* MTAP has broader substrate specificity when compared with the mammalian MTAP [4]. Furthermore, HETA, a non-toxic MTA analog was shown to cure *T. brucei*-infected mice [24,25]. The native MTAP of *T. cruzi* (TcMTAP) has been partially characterized,

showing a molecular mass of 68-kDa, as determined by gel filtration chromatography [26].

In this study we report the identification and characterization of the gene encoding for TcMTAP (*Tcmtap*). The amino acid deduced sequence of TcMTAP shares significant identity with other MTAPs. The gene was cloned and expressed in heterologous system allowing substrate characterization, kinetic constants calculation and determination of optimal temperature and pH. Its biochemical and enzymatic properties lead us to consider TcMTAP a member of PNP/MTAP family 2. TcMTAP is differentially expressed by the three developmental forms of *T. cruzi*. Next, we showed that the enzyme recovers its structure and function after chemical denaturation and assembles into dimer in non-reducing environment.

RESULTS AND DISCUSSION

The TcMTAP belongs to the MTAP/PNP family 2

The *Tcmtap* gene was identified through screening of a *T. cruzi* cDNA library with a specific probe and its sequence contains an ORF of 921 bp that encodes a predicted 307 amino acid protein with a calculated molecular mass of 33,184 Da (Fig. 1). The functional identification of *Tcmtap* is corroborated by the presence, in the translated gene sequence, of the PNP/MTAP family 2 domain signature [LIVF] - x[7] - [GS] - x(2) - H - x - [LIVMFY] - x(4) - [LIVMF] - x[7] - [ATV] - x(1,2) - [LIVM] - x - [ATV] - x(4) - [GN] - x(3,4) - [LIVMF](2) - x(2) - [STN] - [SAGT] - x - G - [GS] - [LIVM]. Multiple amino acid sequence alignment shows that TcMTAP shares high identity with its kinetoplastid counterparts, 59% with *T. brucei* and 58% with *Leishmania major*. The enzyme also exhibits considerable identity with hyperthermophilic MTAPs, sharing 33% and 31% identity with *Sulfolobus solfataricus*

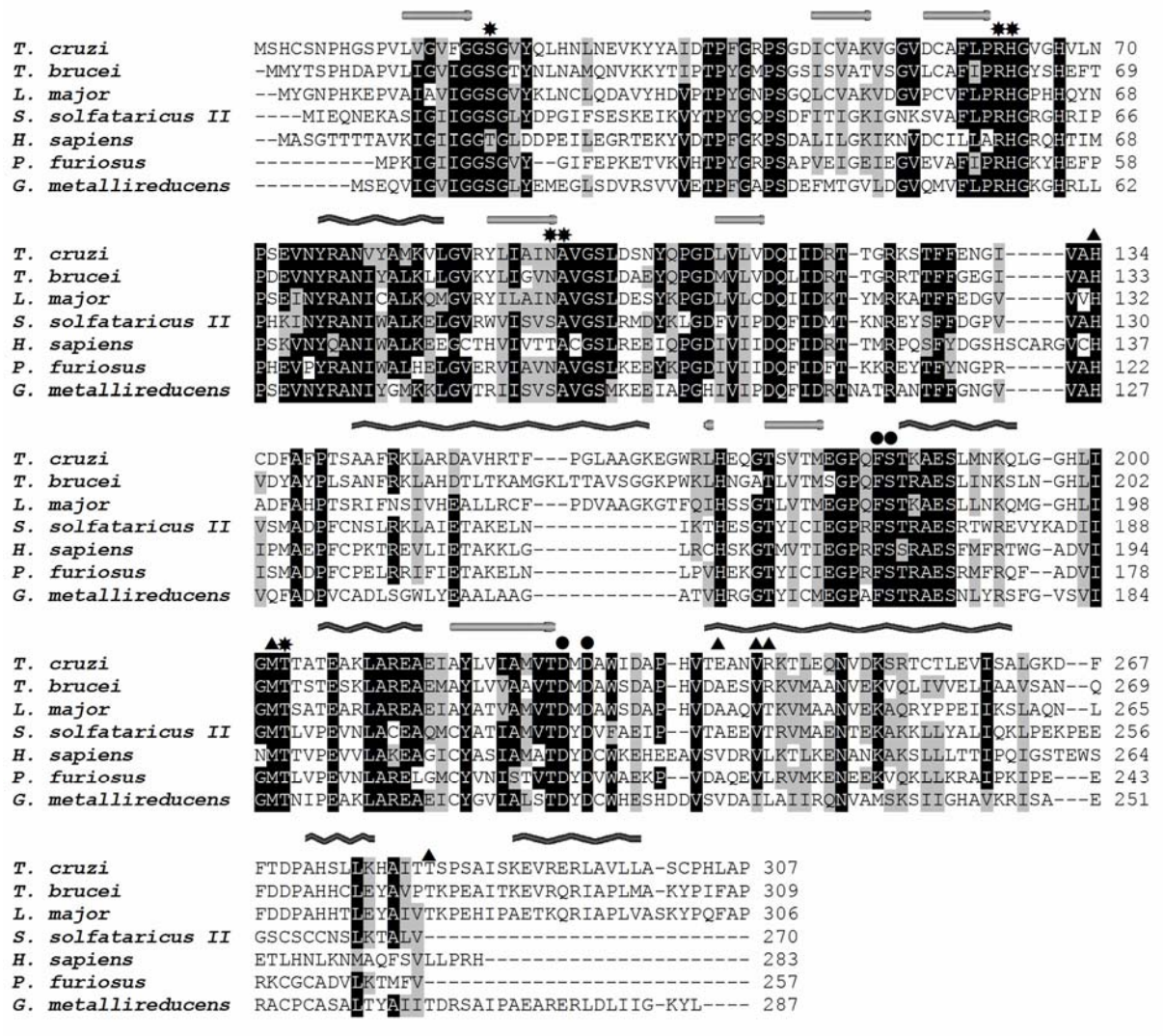

Fig. 1. Comparison of sequence and secondary structure of *T. cruzi* MTAP to other members of MTAP/PNP family 2. All proteins show at least 30% identity with TcMTAP. Proteins' accession number are: AAN46742 (*Trypanosoma cruzi*), XP_823815 (*Trypanosoma brucei*), CAB75631 (*Leishmania major*), NP_343704 (*Sulfolobus solfataricus*), NP_002442 (*Homo sapiens*), NP_577745 (*Pyrococcus furiosus*) and YP_385627 (*Geobacter metallireducens*). The alignment was performed with Clustal W. The identical residues are shaded in black and the similar ones are in gray. The positions at the phosphate (*asterisk*), methylthioribose (*triangle*), and base (*circle*) binding sites of hMPTAP are indicated. The light gray arrows above the sequence indicate alpha-helix and the dark gray waves indicate beta-sheet secondary structures predicted by Jpred (www.compbio.dundee.ac.uk/~www-jpred). The gaps between the structures are consisted of random-coil structures.

and *Pyrococcus furiosus* enzymes, respectively, while it is only 35% identical with human MTAP. Our sequence is almost identical, nine amino acids differing, to the sequences from the TIGR *T. cruzi* genome project (data not show; http://www.tigr.org/tdb/e2k1/tca1/; accession number XM_814834). The presented differences are probably because we sequenced the gene from Berenice stock whereas the genome sequences are from the hybrid CL. Brener, which is heterozygous at many loci [27]. The *Tcmtap* organization in the *T. cruzi* genome was verified by Southern blot analysis. A single band was revealed when the genomic DNA was digested with *Eco*RI, *Kpn*I or *Not*I and probed with the full-length *Tcmtap* (Fig. 2). Differently, when the DNA was digested with *Pst*I and *Xho*I enzymes, the probe hybridized with two bands. This pattern correlates well with sites for *Pst*I and *Xho*I at position 14 and 734 at the gene sequence, respectively. These results suggest that the *Tcmtap* gene is represented as a single copy per haploid genome of the parasite.

The active site of human MTAP (hMTAP) [12] is divided in three specialized parts: phosphate-, pentose-, and base-binding sites. The amino acid residues involved in these three parts of hMTAP active site are present in the sequences of other MTAPs (Fig. 1). Since the base-binding region is completely conserved among MTAPs, we speculate that these enzymes may share substrate specificity towards MTA. The phosphate- and methylthioribose-binding sites of hMTAP are also conserved among the MTAPs but few conservative substitutions occur. Then, we asked whether TcMTAP also shares secondary structure with other MTAPs. The consensus prediction of α-helix and β-sheet structures is shown in Fig. 1. Extended loops, characteristic to all PNPs, link the secondary structural elements and form the contacts between the monomers can be observed. The β-sheets form the monomer core, known to be similar throughout the PNP family, and the α-helices usually surround the monomer. Although sequence

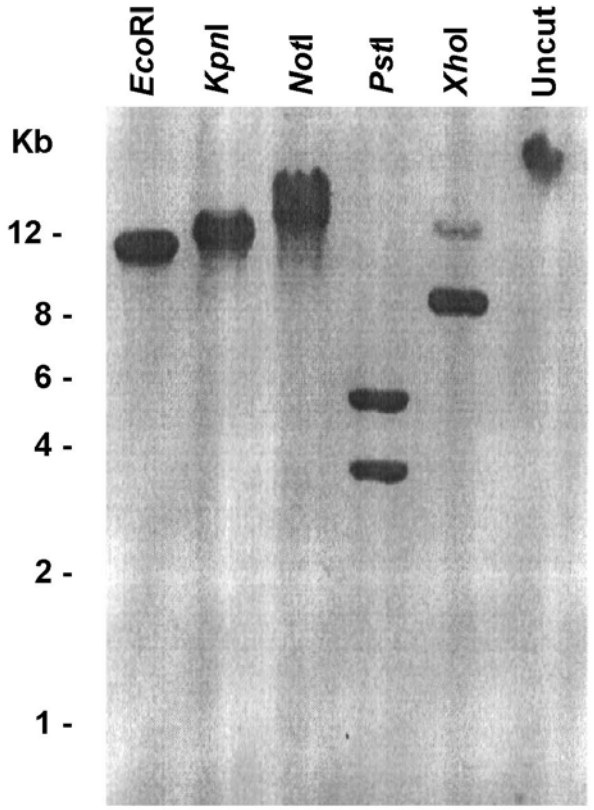

Fig. 2. *Tcmtap* is a single-copy gene. Southern blot of *T. cruzi* genomic DNA digested with *Eco*RI, *Kpn*I, *Not*I, *Pst*I or *Xho*I was performed using a *tcmtaf* cDNA probe. The probe revealed two bands at *Pst*I and *Xho*I lanes as expected by the analysis of *Tcmtap* sequence.

homology is low or nil, structural similarity is quite high among PNPs [20]. It has been postulated (Pugmire, 2002) that sequence divergence and structure similarity may be consequence of a divergent evolutionary event in ancient PNP fold. This common ancestor had probably accepted a wide range of nucleosides substrates, becoming more specialized over time, a specialization observed in eukaryotic organisms. In conjunction, these results indicate that TcMTAP is a member of the MTAP/PNP family 2.

rTcMTAP monomer shows 33-kDa mass

The soluble recombinant TcMTAP (rTcMTAP) was expressed in *E. coli* upon induction with IPTG at 37 °C, yielding approximately 1 mg of protein per liter of culture. The purified rTcMTAP presented an expected apparent molecular mass of 33 kDa under reducing conditions (Fig. 3, Lane 6). This observation led us to ask whether this enzyme would form a dimer, since its native form has been characterized as a 68-kDa protein [26]. To answer this question, we subjected rTcMTAP to electrophoresis in absence of β-mercaptoethanol or DTT. A 66 kDa and higher bands were revealed, while the 33 kDa band migrated more rapidly down the gel with respect to its reduced form (Fig. 4, panel A). To confirm that high bands that appeared in the gel under nonreducing conditions corresponded to oligomers of rTcMTAP, protein bands from a replica of the gel were transferred to a nitrocellulose membrane followed by Western blotting assay. The anti-rTCMTAP antibodies identified the same pattern of protein bands observed in the corresponding Coomassie blue stained gel, thus confirming the rTcMTAP oligomerization (Fig. 4, panel B). These facts suggest that disulfide bonds are positioned inter and intrachain. Then, we speculate that the interchain disulfide bonds link multiple numbers of the enzyme monomer forming the higher bands and that the intrachain bond is responsible for the altered electrophoretic pattern of the 33-kDa

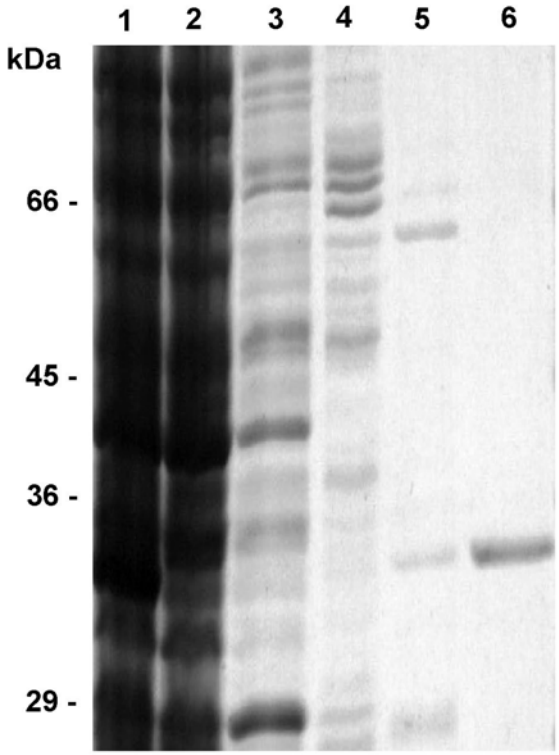

Fig. 3. Electrophoretic analysis of recombinant TcMTAP expression and purification. Lane 1, E. coli BL21 transformed with pET-MTAP after induction with IPTG, crude extract; lane 2, Affinity chromatography purification, non-ligated fraction; lane 3, Fraction after wash with equilibrate buffer, containing 5 mM imidazole; lane 4, Fraction after wash with wash buffer, containing 60 mM imidazole; lane 5, Fraction after wash with buffer containing 100 mM imidazole; lane 6, elution of TcMTAP with buffer containing 400 mM imidazole.

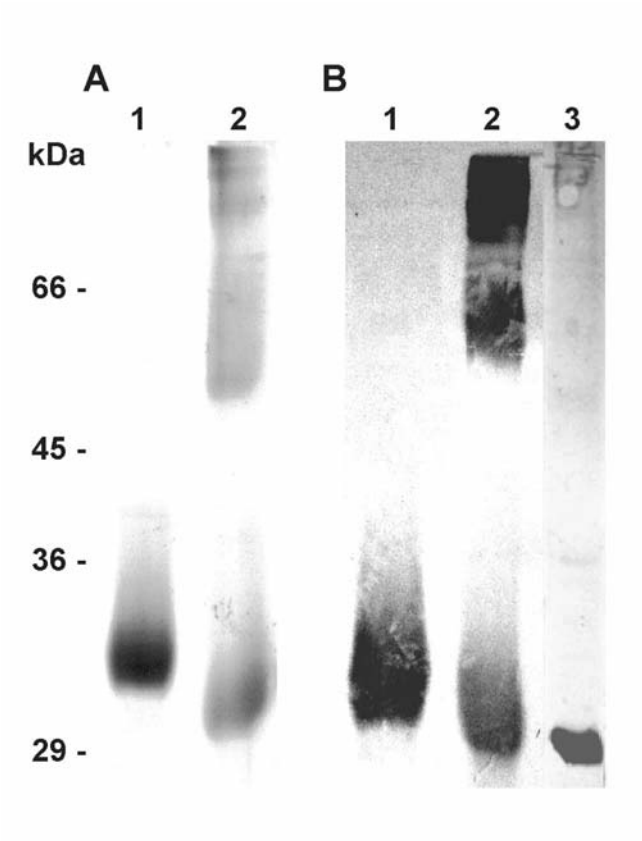

Fig. 4. Recombinant TcMTAP assembles into oligomers. Panel A: SDS-PAGE 10% gel - Lane 1, reduced rTcMTAP; lane B nonreduced rTcMTAP. Panel B: Western-blot of an identical gel from panel A plus epimastigote crude extract - Lane 1, reduced rTcMTAP; Lane 2, nonreduced rTcMTAP.; Lane 3, nonreduced epimastigote crude extract.

monomer. Similar phenomenon was reported in the heterologous expression of MTAP from *S. solfataricus* [28]. A factor contributing to this issue is the inability of bacteria to attain an entire gamut of post-translational modifications a protein requires. An example and most important in our case, the formation of intra- or intermolecular disulfide bonds do not occur in the reducing cytoplasm of *E. coli*, where the recombinant proteins are stored in absence of a secretion signal [29]. Considering that during purification the rTcMTAP faces an oxidative environment that facilitates the formation of disulfide bonds, we added the reducing agent DTT to perform activity assays intending to avoid misplaced disulfide bonds influencing the kinetics measurements.

Native TcMTAP shows 30-kDa mass

The specificity of polyclonal antibodies raised against rTcMTAP was tested against *E. coli* total protein extract and identified a single band, corresponding to the enzyme expected mass (data not shown). Western blotting performed with *T. cruzi* epimastigote crude extract, under non-reducing condition, revealed a single 30-kDa band after probing with anti-rTcMTAP antibodies, but not with pre-immune serum (Fig. 4, panel B lane 3). The mass difference between the recombinant and native proteins is in accordance with the mass of 10 histidines plus 13 other amino acid residues added to the rTcMTAP by plasmid pET19b. To confirm that the protein recognized by the antiserum was indeed the heterologous TcMTAP, an anti-His-tag antibody was tested, recognizing the expected 33 kDa band in the bacteria crude extract upon induction with IPTG (data not shown). From the data presented we assume that native TcMTAP does not form an oligomer with subunits maintained by disulfide bonds since Western blotting under nonreducing conditions showed a single 30-kDa band. Conceivably, a possible oligomer could be formed by weak interactions that were unable to resist the SDS-PAGE environment. This could explain the reported 68-kDa molecular mass of

native TcMTAP that was estimated by gel filtration [26]. Regarding this issue, previous reports on PNPs have showed problems defining molecular mass and subunit composition based on electrophoresis, gel filtration and other low resolving methods [20]; for e.g. a dimer composition had been proposed to the human erythrocyte PNP based on gel filtration and sedimentation equilibrium assays [30], but it has been considered obsolete since the establishment of its trimeric structure in crystal (PDB 1ULA). A reasonable explanation for this incongruence is the existence of an equilibrium mixture of species with different subunit composition when the protein is in solution, previously reported fact in PNP family [20].

TcMTAP is differentially expressed through *T. cruzi*'s developmental stages

Levels of TcMTAP expression throughout the life cycle of *T. cruzi* were assayed by Western-blotting the three parasite developmental stages (10^7 parasites per immunoblot lane) using the raised serum. The antibodies were able to recognize the native MTAP in the three forms of the parasite (Fig. 4). As judged by this assay, the free living tripomastigote and epimastigote forms express similar amounts of TcMTAP while the intracellular amastigotes display a significantly lower quantity. A possible explanation is that amastigotes obtain access to methionine and purine pools from the host cell and the active transport fulfills part of its requirement for these compounds. In opposite, the amount of adenosine is quite low in human plasma [31], leading the extracelullar forms, in order to satisfy their purine requirement, to induce the expression of the purine salvage pathway proteins. These results show that MTAP is differentially expressed in *T. cruzi* life cycle.

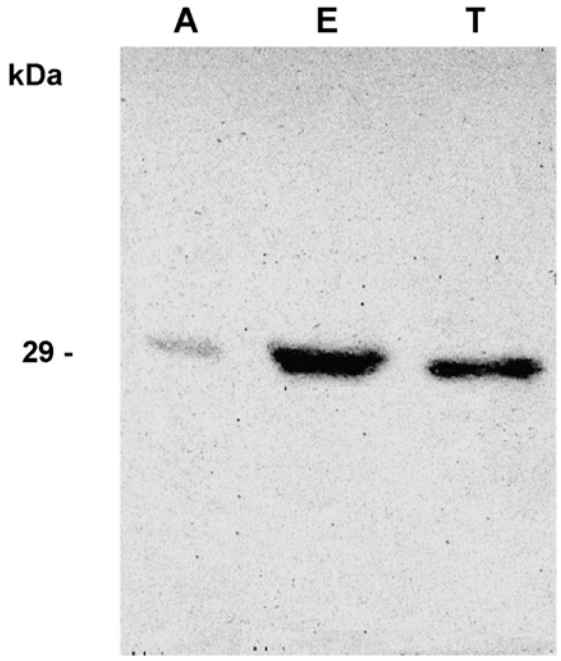

Fig. 5. TcMTAP is differently expressed by *T. cruzi* developmental forms. Native MTAP was identified in the 3 different forms of the parasite using anti-rTcMTAP antibodies. Total extract of 10^7 parasites of each form was applied at the lanes. Lane **A**: amastigote; lane **E**: epimastigote and lane **T**: trypomastigote.

Enzymatic Assay

To test the recombinant TcMTAP activity and to calculate the kinetics constants, a spectrophotometric assay was employed to measure the conversion of MTA into adenine as previously reported [32]. The temperature dependence of rTcMTAP activity assayed in the range from 37 °C to 80 °C is reported in Fig. 6. The enzyme appears moderately thermophilic, showing an optimal temperature of 50 °C, keeping 35% activity at 70 °C. Thermostability is a common characteristic among PNPs from thermophilic and non-thermophilic organisms, e.g. *E. coli* PNP is stable for 10 min at 55 °C [33] and that of *Klebsiella* for 16 h at 60 °C [34]. Forterre [35] has postulated that the mesophilic prokaryotes existing today must have evolved through a gradual adaptation of thermophilic enzymes to lower temperature optima. The presence of thermophilic enzymes may represent an evolutionary holdover from a thermophilic ancestor. We also tested the pH effect on MTA phosphorolysis (Fig. 7). It was shown that the enzyme has a dependence on neutral pH but maintains its activity over a broad pH range. Although maximum activity was observed at pH 7.4, the measured enzymatic activities at pH 5.0 and 8.0 were 51 and 78 % of the optimal. These findings are in accordance with the results obtained for the native enzyme [26]. Furthermore, PNPs, with few exceptions, show broad pH activity [20].

The kinetics parameters of rTcMTAP for phosphate and MTA substrates were determined at 37 °C that is closer to the natural conditions encountered at the mammal host. The K_m, k_{cat} and k_{cat}/K_m values for the substrates MTA and phosphate were calculated and typical Michaelis-Menten kinetics were observed (Table 1). In previous reports the K_m and substrate specificity from the partially purified native *T. cruzi* and *T. brucei* MTAPs were calculated [22,26], exhibiting a K_m of 3 and 2 μM for MTA substrate, respectively. These results are considerably divergent from the K_m of 48 μM

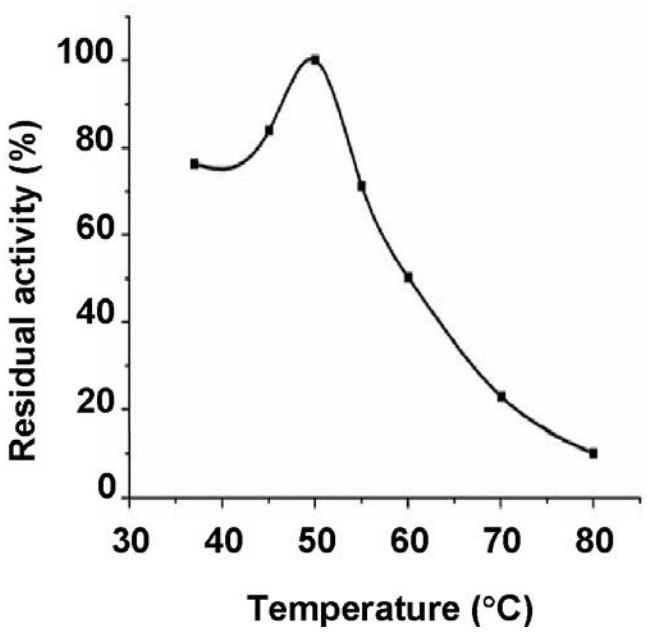

Fig. 6. rTcMTAP exhibited maximum activity at 50 °C. The effect of temperature on recombinant TcMTAP activity was determined, revealing a possible heritage from a thermophilic ancestor. Activity rapidly drops above 50 °C.

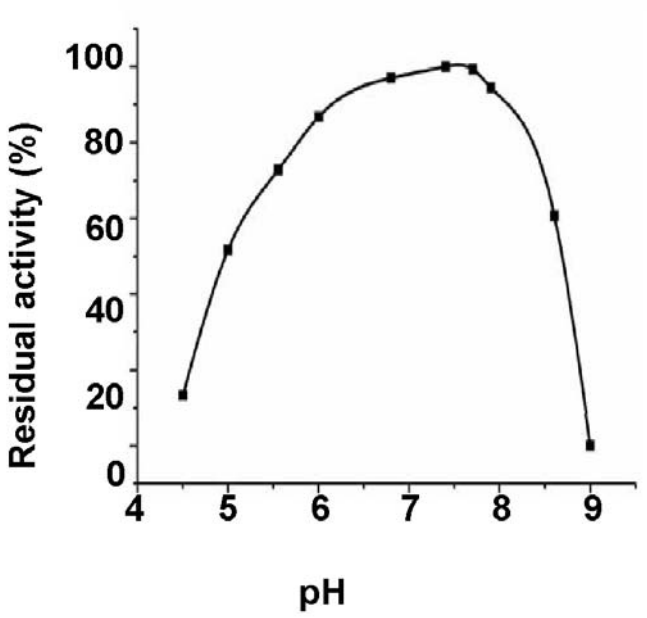

Fig. 7. rTcMTAP is active over a broad pH range. Enzyme maximum activity was observed at 7.4, whereas maintaining high activity in the neighborhood. The activity observed at pH 7.4 is expressed as 100%.

for MTA of the recombinant enzyme. This affinity difference between the native and recombinant enzymes may be due to the fact that the native proteins were partially purified from the parasite extract, allowing a masked promiscuous nucleoside phosphorylase to alter the rates. The substrate specificity results were very similar between the native enzymes and rTcMTAP, being MTA the preferred substrate in all cases.

The enzyme shows an increasing affinity for MTA when the pH moves towards 7.4 (K_m 48.1 μM) as compared to pH 5.0 (K_m 162 μM) and 6.0 (K_m 83.2 μM). The increasing affinity is expected since pH 7.4 is the optimal and, most likely, at this condition intra chain interactions are at their best configuration and the protein is more stabilized. The K_m for the substrate phosphate was almost identical to that of MTA, indicating no preference in the order of substrate binding.

Elucidating substrate specificity is an important step towards the classification of the enzyme as a member of the MTAP family and to identify the major substrate characteristics that should be considered when searching for specific inhibitors. Thus, the substrate specificity of rTcMTAP was determined by incubating the purified enzyme with MTA, inosine, guanosine, adenosine or 2'-deoxyadenosine (Table 2). The enzyme catalyzed the phosphorolysis of MTA with the highest specific activity. It cleaved adenosine and deoxy-adenosine with similar specific activity. Nevertheless, the enzyme showed a limited activity on Guo and failed to cleave Ino. These results correlate well with the idea that while human MTAP is very specific for 6-aminopurine nucleosides, its counterparts from microorganisms usually show broader substrate specificity, cleaving other molecules like 6-oxopurine nucleosides, Guo and Ino [22,24,36].

Table 1. Kinetic parameters of rTcMTAP. Kinetics parameters against MTA and phosphate were determined at 37 °C at different pH.

Substrate	pH	K_m (μM)	k_{cat} (s^{-1})	k_{cat}/K_m ($s^{-1}.\mu M^{-1}$)
MTA	5.0	162	4.3	2.7×10^{-2}
	6.0	83.1	5.2	6.3×10^{-2}
	7.4	48.1	6.9	1.4×10^{-1}
Phosphate	7.4	55.4	8.6	1.5×10^{-1}

Table 2. Substrate specificity of rTcMTAP against nucleosides substrates. *N.d.* non detected. Rates were normalized by setting the rate of MTA cleavage at 100%. The actual rate was 2.2 μmoles/ min.mg protein.

Substrate	Relative rate of cleavage (%)
MTA	100
Adenosine	83
Deoxy-adenosine	78
Inosine	*N.d.*
Guanosine	32

rTcMTAP reassumes its native structure after denaturation.

To analyze the rTcMTAP capability of renaturation, we first incubated the enzyme in the presence of 6 M guanidine-HCl during 24 h at 25 °C. The denaturation was evaluated by monitoring the shift in fluorescence maximum wavelength upon excitation at 295 nm. In the folded state the protein exhibited relative fluorescence emission maximum at 333 nm, which is considered a characteristic of tryptophan that is in a low-polar hydrophobic environment (Fig. 8, slope A) [37]. After denaturation, the fluorescence showed a large red shift due to the increased exposure of the tryptophanyl residues to the more polar aqueous environment (Fig. 8, slope C). The refolding process was started by 20-fold dilution of the sample. Extensive dialyses were performed until complete removal of the denaturant. The refolding process was monitored by fluorescence measurements and activity assays. After refolding, rTcMTAP exhibited a fluorescence spectrum with almost the same profile as the native protein, i.e. a fluorescence maximum emission at 337 nm (Fig. 8, slope B). The refolded enzyme activity was 51% of the control protein. On the basis of the reported data, we conclude that rTcMTAP can recover its fluorescence spectrum to that prior to the unfolding process, which can be also associated with recovered tertiary structure. The MTAP of *P. furiosus* subjected to a similar experiment also exhibited a fluorescence spectrum with the same features as the native enzyme after the refolding process [38]. Nevertheless, the *P. furiosus* protein only exhibited the correct spectrum when the denaturation process was carried out in the presence of reducing agents, which led us to assume that intact disulfide bonds in rTcMTAP do not interfere with the refolding process.

Although functional properties for TcMTAP are unknown, activities of MTAPs are essential for the survival of African trypanosomes and *Leishmania*, thus, considered

good targets for drugs [23]. Since a biosynthetic pathway is lacking, *T. cruzi* must acquire purine ring through host and endogenous metabolite recycling. Then, inactivation of TcMTAP by specific inhibitors or through gene disruption would reveal its function in both *T. cruzi* biology and pathogenesis of Chagas disease. The molecular and biochemical features of TcMTAP presented here and further investigations would contribute to rational development of leads aiming at chemotherapy of *T. cruzi* infections.

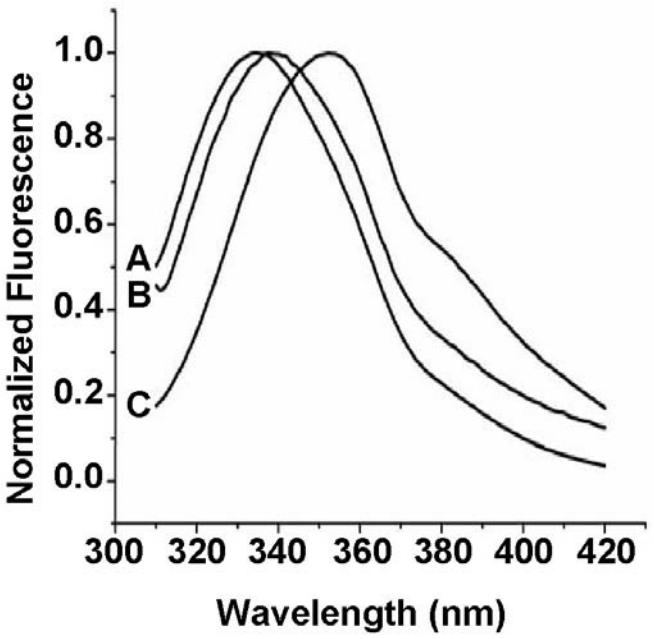

Fig. 8. Recombinant TcMTAP recovers native folding after chemical denaturation. After 24 h incubation at 25 °C rTcMTAP fluorescence emission spectrum was recorded as follows: (A) native enzyme in 20 mM Tris/HCl, pH 7.4; (B) refolded enzyme, after denaturant removal; (C) unfolded enzyme in 6 M Gnd-HCl.

MATERIALS AND METHODS

Parasites

*T. cruz*i epimastigote forms from Berenice stock were grown in liver infusion tryptose medium supplemented with 100 units/ml penicillin, 100 μg/ml streptomycin and 10 % (v/v) fetal calf serum at 28 °C with continuous agitation. Trypomastigote and amastigote forms of the parasite were obtained by monolayer culture of murine muscle L-6 cells grown in RPMI medium containing 10 % fetal calf serum at 37 °C in 5 % CO2 and then purified as described previously [39,40].

Cloning and expression of *T. cruzi* MTAP

The *Tcmtap* gene was identified upon screening a cDNA library with serum from *T. cruzi*-infected rabbit as described (Caetano MAI, Garcia M MBP) and completely sequenced on both sides. Specific primers $MTAP_1$ (forward, 5′-cgcgagCAT**ATG**TCCCACTGCAGCATTCCAC-3′; lowercase, random bases; underlined, *Nde*I site; bold, initiation codon) and $MTAP_2$ (reverse, 5′-cacagaCTCGAGCAA**TCA**TGGGGCGAGATGCGGG-3′ lowercase, random bases; underlined, *Xho*I site; bold, stop codon) were synthesized. *T. cruzi* cDNA was synthesized using total RNA primed with oligo(dT) and mini-exon primers to assure amplification of complete and spliced mRNAs (Thermoscript RT-PCR system, Invitrogen). Then, the cDNA product was used to amplify the complete ORF with primers $MTAP_1$ and $MTAP_2$ using Platinum *Taq* DNA polymerase high fidelity (Invitrogen). The PCR product was subsequently cloned into pGEM-T-easy vector (Promega) and completely sequenced on both directions. The ORF was removed from the vector using *Nde*I enzyme and subcloned into a previously *Nde*I-digested pET19b plasmid (Novagen), generating pTcMTAP, and the correct orientation of the gene was

confirmed by sequencing. Secondary structure of the protein was predicted by submitting its primary sequence to the Jpred server (http://www.compbio.dundee.ac.uk/~www-jpred/). The N-terminal His tagged TcMTAF was expressed in *E. coli* BL21(DE3) strain at 37 °C upon induction with 1 mM isopropyl-β-D-thiogalactoside (IPTG) during 5 h. Cells were harvested by centrifugation, lysed with Bugbuster™ (Novagen) and cell debris were removed by centrifugation at 20,000 *g* for 20 min at 4 °C.

The recombinant protein was purified with the His-Bind resin and buffer kit (Novagen). The bacterial protein extract supernatant was loaded on a nickel charged column previously equilibrated with binding buffer. After the non-ligated proteins were eluted, the contaminant proteins were washed away from the column with 10 volumes of binding buffer, then with 3 volumes of washing buffer, and a final wash containing 100 mM imidazole. Finally, the His_{10} N-terminal tagged MTAP was eluted with 6 volumes of elution buffer, containing 400 mM imidazole. After dialysis against 10 mM Tris-HCl pH 7.4 overnight at 4 °C, the purified protein was concentrated with a Centricon 10 (Millipore). The protein concentration was determined by measuring A_{280} using the predicted extinction coefficient of 21980 M^{-1} cm^{-1}, calculated with ProtParam tool (http://www.expasy.org/tools/protparam.html). The cDNA sequence of TcMTAP is available in GenBank® under the accession number AY144609.

Enzymatic assay

The activity of TcMTAP was spectrophotometrically determined by measuring the conversion of MTA into adenine as a decrease in absorbance at 275 nm to give Δε between MTA and adenine of 1.6 mM^{-1} cm^{-1} [32]. The activity assays were performed by incubating 160 nM TcMTAP in 100 mM K-phosphate buffer pH 7.4 containing 2

mM DTT (reaction buffer) and 250 μM MTA at 37 °C. The optimal pH of TcMTAP activity was assayed as above in the following 100 mM buffers: Na-acetate pH 4.5 and 5.0, Na-citrate pH 5.6, Bis-Tris pH 6.0 and 6.8, K-phosphate pH 7.4 (no phosphate added), HEPES pH 7.7 and 7.9, Bicine pH 8.6, and Tris-HCl pH 9.0. To determine rTcMTAP optimal temperature activity, the reactions were performed at 37, 45, 50, 55, 60, 70, or 80 °C. The reaction mixture to calculate the K_m and V_{max} for MTA (20 – 333 μM) and phosphate substrates (50 – 2,200 μM) were reaction buffer and 100 mM Hepes pH 7.4, 2 mM DTT and 500 μM MTA, respectively. The kinetics parameters were calculated using a nonlinear regression of Michaelis-Menten equation in a Beckman Coulter spectrophotometer DU640 equipped with a temperature control system. All constants have a $p < 0.05$.

Activity against 1 mM adenosine (Ado), 1 mM inosine (Ino), 1 mM 2'-deoxyadenosine (dAdo) or 0.04 mM guanosine (Guo) substrates was measured in a xanthine oxidase-coupled spectrophotometric assay [41,42]. This assay was carried out as described above in reaction buffer containing 0.1 UI xanthine oxidase /mL. The extinction coefficient for Ado and dAdo is 15.5, 12.0 for Ino and -4.2 mM^{-1} cm^{-1} for Guo, monitored at 305, 293 and 255 nm, respectively [41]. The reactions were initiated by addition of purified recombinant TcMTAP.

Anti-TcMTAP antiserum production

Polyclonal antibodies against *T. cruzi* MTAP was generated by subcutaneous inoculation of the purified recombinant protein into New Zealand rabbit. Pre-immune blood was drawn prior to the initial immunization, and the serum was used as a negative control. The recombinant protein, 20 μg in 100 μL of PBS, was mixed and emulsified in an equal volume of Freund's complete adjuvant (Sigma Chemical Co.) and injected in the rabbit. Two subsequent injections were given at intervals of 2 weeks with the

enzyme in incomplete adjuvant, followed by a final booster with the enzyme alone. Sera were stored at - 20 °C in the presence of 50% glycerol.

Immunobloting

Soluble protein extracts (20 µg) from IPTG-induced BL21 bacteria either carrying pTcMTAP or empty vector, purified rTcMTAP or total proteins from amastigotes, epimastigotes or trypomastigotes of *T. cruzi*, corresponding to 1×10^7 cells/well, were subjected to SDS-PAGE (10 % polyacrylamide) under reducing conditions. Parasites were solubilized directly in the electrophoretic sample buffer. Proteins were transferred on to a nitrocellulose membrane and blocked by incubation in 5 % (w/v) non-fat milk/PBS overnight at 4 °C. Blots were incubated for 2 h with control or anti-rTcMTAP serum diluted in 1 % non-fat milk/PBS. After three washes of 5 min each with PBS, membranes were incubated for 2 h with alkaline phosphatase-conjugated goat anti-rabbit IgG (Zymed) diluted to 1:2000, washed as above, and the immunocomplexes were revealed with the alkaline-phosphatase substrate 5-bromo-4-chloro-3-indolyl-1-phosphate /Nitro Blue Tetrazolium (Promega).

Refolding

Fluorescence emission spectra of TcMTAP tryptophans 167 and 230 were used to monitor changes in the environment of these residues upon the unfolding of the protein. Intrinsic fluorescence emission measurements were carried out on an Aminco Bowman Series 2 (SLM Aminco) luminescence spectrometer using a 1×1 cm path length cuvette. Fluorescence emission spectra were recorded at 310-420 nm at the controlled temperature of 25 °C, recording the excitation wavelength of 295 nm. For unfolding, rTcMTAP (final concentration 2.0 mg/ mL) was incubated for 24 h at 25 °C

in the absence or presence of 6 M Gnd-HCl in 20 mM K-phosphate pH 7.4. The unfolding process was followed by changes in fluorescence emission. After 24 h, the emission spectra were recorded; refolding was started by 20-fold dilution of the samples in 20 mM K-phosphate pH 7.4 at 25 °C. The final concentration of Gnd-HCl in the renaturation mixture was 0.3 M, whereas the protein concentration was 90 μg/mL. The samples were extensively dialyzed against 20 mM K-phosphate pH 7.4 until complete removal of Gnd-HCl, and then activity measurements under standard conditions and fluorescence emission spectra were recorded. Experiments were normalized in accordance with protein concentration before and after renaturation and buffer fluorescence emission were subtracted [38].

REFERENCES

[1] Prata A (2001). Clinical and epidemiological aspects of Chagas disease. *Lancet Infect Dis* **1**, 92-100.

[2] Urbina JA (2001). Specific treatment of Chagas disease: current status and new developments. *Curr Opin Infect Dis* **14**, 733-741.

[3] Bacchi CJ, Goldberg B, Rattendi D, Gorrell TE, Spiess AJ & Sufrin JR (1999). Metabolic effects of a methylthioadenosine phosphorylase substrate analog on African trypanosomes. *Biochem Pharmacol* **57**, 89-96.

[4] Bacchi CJ & Yarlett N (2002). Polyamine metabolism as chemotherapeutic target in protozoan parasites. *Mini Rev Med Chem* **2**, 553-563.

[5] Marasco CJ, Jr., Kramer DL, Miller J, Porter CW, Bacchi CJ, Rattendi D, Kucera L, Iyer N, Bernacki R, Pera P & Sufrin JR (2002). Synthesis and evaluation of analogues of 5'-([(Z)-4-amino-2-butenyl]methylamino)-5'-deoxyadenosine as inhibitors of tumor cell growth, trypanosomal growth, and HIV-1 infectivity. *J Med Chem* **45**, 5112-5122.

[6] Byers TL, Casara P & Bitonti AJ (1992). Uptake of the antitrypanosomal drug 5'-([(Z)-4-amino-2-butenyl]methylamino)-5'-deoxyadenosine (MDL 73811) by the purine transport system of Trypanosoma brucei brucei. *Biochem J* **283 (Pt 3)**, 755-758.

[7] Tolbert WD, Ekstrom JL, Mathews, II, Secrist JA, 3rd, Kapoor P, Pegg AE & Ealick SE (2001). The structural basis for substrate specificity and inhibition of human S-adenosylmethionine decarboxylase. *Biochemistry* **40**, 9484-9494.

[8] Berger BJ, Carter NS & Fairlamb AH (1993). Polyamine and pentamidine metabolism in African trypanosomes. *Acta Trop* **54**, 215-224.

[9] Goldberg B, Yarlett N, Rattendi D, Lloyd D & Bacchi CJ (1997). Rapid methylation of cell proteins and lipids in Trypanosoma brucei. *J Eukaryot Microbiol* **44**, 345-351.

[10] Sufrin JR, Meshnick SR, Spiess AJ, Garofalo-Hannan J, Pan XQ & Bacchi CJ (1995). Methionine recycling pathways and antimalarial drug design. *Antimicrob Agents Chemother* **39**, 2511-2515.

[11] Goldberg B, Rattendi D, Yarlett N, Lloyd D & Bacchi CJ (1997). Effects of carboxylmethylation and polyamine synthesis inhibitors on methylation of Trypanosoma brucei cellular proteins and lipids. *J Eukaryot Microbiol* **44**, 352-358.

[12] Appleby TC, Erion MD & Ealick SE (1999). The structure of human 5'-deoxy-5'-methylthioadenosine phosphorylase at 1.7 A resolution provides insights into substrate binding and catalysis. *Structure* **7**, 629-641.

[13] Williams-Ashman HG, Seidenfeld J & Galletti P (1982). Trends in the biochemical pharmacology of 5'-deoxy-5'-methylthioadenosine. *Biochem Pharmacol* **31**, 277-288.

[14] Ceron CR, Caldas RD, Felix CR, Mundim MH & Roitman I (1979). Purine metabolism in trypanosomatids. *J Protozool* **26**, 479-483.

[15] Berens RL KE, Marr JJ (1995) in: *Biochemistry and molecular biology of parasites.*, pp. 89-117 (M, M.J.a.M., Ed.) Academic Press, London.

[16] Carter NS & Fairlamb AH (1993). Arsenical-resistant trypanosomes lack an unusual adenosine transporter. *Nature* **361**, 173-176.

[17] Goldberg B, Rattendi D, Lloyd D, Sufrin JR & Bacchi CJ (2001). In situ kinetic characterization of methylthioadenosine transport by the adenosine transporter (P2) of the African Trypanosoma brucei brucei and Trypanosoma brucei rhodesiense. *Biochem Pharmacol* **61**, 449-457.

[18] Hammond DJ & Gutteridge WE (1984). Purine and pyrimidine metabolism in the Trypanosomatidae. *Mol Biochem Parasitol* **13**, 243-261.

[19] Marr JJ (1991). Purine analogs as chemotherapeutic agents in leishmaniasis and American trypanosomiasis. *J Lab Clin Med* **118**, 111-119.

[20] Bzowska A, Kulikowska E & Shugar D (2000). Purine nucleoside phosphorylases: properties, functions, and clinical aspects. *Pharmacol Ther* **88**, 349-425.

[21] Pugmire MJ & Ealick SE (2002). Structural analyses reveal two distinct families of nucleoside phosphorylases. *Biochem J* **361**, 1-25.

[22] Ghoda LY, Savarese TM, Northup CH, Parks RE, Jr., Garofalo J, Katz L, Ellenbogen BB & Bacchi CJ (1988). Substrate specificities of 5'-deoxy-5'-methylthioadenosine phosphorylase from Trypanosoma brucei brucei and mammalian cells. *Mol Biochem Parasitol* **27**, 109-118.

[23] el Kouni MH (2003). Potential chemotherapeutic targets in the purine metabolism of parasites. *Pharmacol Ther* **99**, 283-309.

[24] Bacchi CJ, Sufrin JR, Nathan HC, Spiess AJ, Hannan T, Garofalo J, Alecia K, Katz L & Yarlett N (1991). 5'-Alkyl-substituted analogs of 5'-methylthioadenosine as trypanocides. *Antimicrob Agents Chemother* **35**, 1315-1320.

[25] Bacchi CJ, Sanabria K, Spiess AJ, Vargas M, Marasco CJ, Jr., Jimenez LM, Goldberg B & Sufrin JR (1997). In vivo efficacies of 5'-methylthioadenosine analogs as trypanocides. *Antimicrob Agents Chemother* **41**, 2108-2112.

[26] Miller RL, Sabourin CL & Krenitsky TA (1987). Trypanosoma cruzi adenine nucleoside phosphorylase. Purification and substrate specificity. *Biochem Pharmacol* **36**, 553-560.

[27] Sturm NR, Vargas NS, Westenberger SJ, Zingales B & Campbell DA (2003). Evidence for multiple hybrid groups in Trypanosoma cruzi. *Int J Parasitol* **33**, 269-279.

[28] Cacciapuoti G, Fusco S, Caiazzo N, Zappia V & Porcelli M (1999). Heterologous expression of 5'-methylthioadenosine phosphorylase from the archaeon Sulfolobus solfataricus: characterization of the recombinant protein and involvement of disulfide bonds in thermophilicity and thermostability. *Protein Expr Purif* **16**, 125-135.

[29] Baneyx F & Mujacic M (2004). Recombinant protein folding and misfolding in Escherichia coli. *Nat Biotechnol* **22**, 1399-1408.

[30] Lewis AS & Lowy BA (1979). Human erythrocyte purine nucleoside phosphorylase: molecular weight and physical properties. A Theorell-Chance catalytic mechanism. *J Biol Chem* **254**, 9927-9932.

[31] Hirschhorn R (1985). Complete and partial adenosine deaminase deficiency. Relationship of immune function to metabolite concentrations, enzyme activity, and effects of therapy. *Ann N Y Acad Sci* **451**, 20-25.

[32] Singh V, Shi W, Evans GB, Tyler PC, Furneaux RH, Almo SC & Schramm VL (2004). Picomolar transition state analogue inhibitors of human 5'-methylthioadenosine phosphorylase and X-ray structure with MT-immucillin-A. *Biochemistry* **43**, 9-18.

[33] Krenitsky TA, Koszalka GW & Tuttle JV (1981). Purine nucleoside synthesis, an efficient method employing nucleoside phosphorylases. *Biochemistry* **20**, 3615-3621.

[34] Ling F, Inuoe Y & Kimura A (1994). Induction, purification and utilization of purine nucleoside phosphorylase and uridine phosphorylase from *Klebsiella* sp. *Process biochemistry* **29**, 355-361.

[35] Forterre P (1995). Looking for the most "primitive" organism(s) on Earth today: the state of the art. *Planet Space Sci* **43**, 167-177.

[36] Toorchen D & Miller RL (1991). Purification and characterization of 5'-deoxy-5'-methylthioadenosine (MTA) phosphorylase from human liver. *Biochem Pharmacol* **41**, 2023-2030.

[37] Volotovskii ID & Konev SV (1967). [Relation between the conformation and UV luminescence of proteins]. *Biofizika* **12**, 200-205.

[38] Cacciapuoti G, Moretti MA, Forte S, Brio A, Camardella L, Zappia V & Porcelli M (2004). Methylthioadenosine phosphorylase from the archaeon Pyrococcus furiosus. Mechanism of the reaction and assignment of disulfide bonds. *Eur J Biochem* **271**, 4834-4844.

[39] Ley V, Robbins ES, Nussenzweig V & Andrews NW (1990). The exit of Trypanosoma cruzi from the phagosome is inhibited by raising the pH of acidic compartments. *J Exp Med* **171**, 401-413.

[40] Tardieux I, Webster P, Ravesloot J, Boron W, Lunn JA, Heuser JE & Andrews NW (1992). Lysosome recruitment and fusion are early events required for trypanosome invasion of mammalian cells. *Cell* **71**, 1117-1130.

[41] Miller RL & Lindstead D (1983). Purine and pyrimidine metabolizing activities in Trichomonas vaginalis extracts. *Mol Biochem Parasitol* **7**, 41-51.

[42] Kalckar HM (1947). Differential spectrometry of purine compounds by means of specific enzymes 1. Determination of hydroxypurine compounds. *The Journal of biological chemistry* **167**, 429-443.

THE DRUG TARGET METHYLTHIOADENOSINE PHOSPHORYLASE of *Trypanosoma cruzi* EXHIBITS REMARKABLE RESISTANCE TO THERMAL AND CHEMICAL DENATURATION.

Summary

Methylthioadenosine phosphorylase (MTAP) belongs to the family 2 of purine nucleoside phosphorylase/MTAP, whose members assembles into different oligomeric constitutions. These widely distributed enzymes catalyze the phosphorolysis of MTA, a byproduct of polyamine biosynthesis and are the starting point of purine and methionine salvage pathways. Herein, we report the physicochemical characterization of the MTAP of the trypanosomatid *Trypanosoma cruzi* (TcMTAP) that is considered a potential target for chemotherapy of Chagas disease, an incurable sickness responsible for thousands of deaths in Latin America. Thermal denaturation followed by circular dichroism performed at broad range of pH showed reduced dependence between enzyme stability and environment ionization condition. TcMTAP exhibited striking resistance to thermal denaturation, unfolding only above 79 °C. Its secondary structure content is significantly composed of α-helices, as predicted from circular dichroism data. However, even after thermal denaturation, the content of α-helices showed little variation, markedly at pH 7.4 and 9.0. Chemical denaturation of TcMTAP, induced by guanidine-hydrochloride or urea, was monitored by far-UV circular dichroism and fluorescence spectroscopy. The enzyme kept folded in concentration as high as 3.6 M of guanidine-hydrochloride and 8 M of urea. The thermodynamic parameters calculated from thermal and chemical denaturation assays were in good agreement, $\Delta G(H_2O)$ = 35.5 kcal/mol and ΔG^{25} = 36 kcal/mol. Thermal denaturation carried out in the presence of hexadecyltrimethylammonium (CTAB) increased enzyme stability at pH 6.0. Knowledge of biophysical properties of TcMTAP may aid in understanding its structural behavior in different environment and in interpreting its peculiar biochemical characteristics, thus helping in development of specific inhibitors.

INTRODUCTION

Methylthioadenosine phosphorylase (MTAP; E.C. 2.4.2.28) belongs to the purine nucleoside family 2 (PNP, E.C. 2.4.2.1) and is ubiquitously distributed in nature. It phosphorolytically cleaves the glycosidic bond of the sulfur-containing nucleoside methylthioadenosine (MTA), which is a metabolic product of S-adenosylmethionine (AdoMet) in polyamine biosynthesis. MTA is also the starting point of two major salvage pathways, the purine and methionine ones [1]. MTAP readily metabolizes MTA to adenine and methylthio-ribose-1-phosphate (MTR1P). Adenine will ultimately replenish the AMP and ATP pool whereas MTR1P will be converted to methionine. The MTAP and the intermediates of the pathways associated with MTA recycling have been considered chemotherapy targets against human cancers related with alterations at the chromosomal locus 9p21 and against protozoan diseases such as trypanosomiasis, leishmaniasis and malaria. This is because those cancer cells and protozoa parasites lack the machinery to synthesize the purine ring de novo and, thus, depend on the salvage pathway [2,3]. Differently from human MTAP, that show high specificity for MTA, MTAPs of parasitic protozoa also displays activity on other nucleosides and its analogues [4]. For instance, it has been shown that *Trypanosoma brucei* and *Trypanosoma rhodesiense* are susceptible to the MTA analog, 5'-deoxy-5'-(hydroxyethylthio)adenosine (HETA), which was able to cure trypanosoma-infected mice without damaging mammalian cells [5,6].

Thermodynamic characterization may contribute to explain enzyme's biochemical properties, for example a broad pH range activity, thermostability, and substrate preference [7]. In addition, the biophysical data can also provide insights into the molecular mechanisms related with protein stability, overall structure and biotechnological applicability [8], e. g. protein-ligand affinities, presence of intermediate in the folding/unfolding process and rational drug design [9,10].

The kinetoplastid protozoan *Trypanosoma cruzi* is the etiological agent of Chagas disease, which is a chronic infection highly prevalent in Latin America. The drugs currently used to treat human *T. cruzi* infection neither prevent the chronic phase of the disease nor eliminate the parasite. Although new potential drugs are being evaluated there is an urge to characterize *T. cruzi* virulence factors that could be used as targets for the conception of new molecules to treat this parasitic infection [11]. Purine salvage pathway of *T. cruzi* is considered a feasible drug target since the parasite,

likewise other kinetoplastids, is unable to synthesize the purine ring de novo [4,12,13]. We have biochemically characterized the recombinant purine-salvage-pathway participating enzyme MTAP of *T. cruzi* (rTcMTAP) [14]. The enzyme is active over a broad pH range, displays considerable thermostability and is capable to renature after chemical unfolding. rTcMTAP assembles into oligomers in solution, which apparently is composed by a mixture of association species [14]. Similar results were found by, Wielgus-Kutrowska [15], on *Cellulomonas* sp. PNP.

In this study we calculated the thermodynamic parameters and characterized the structural stability of the recombinant MTAP from *T. cruzi*. rTcMTAP exhibited striking resistance to thermal and chemical denaturation, followed by circular dichroism (CD) and fluorescence spectroscopy. The enzyme unfolds as a two-state model and increases its thermal stability at acid to neutral pH. In addition, the secondary structure content suffers little variation during the thermal unfolding process. We also tested the presence of stabilizers hexadecyltrimethylammonium bromide (CTAB) and sorbitol. which altered the enzyme stability and its denaturation pattern. Until present date, only the *Cellulomonas* sp. PNP [15] had its biophysical parameters fully determined, but no member of MTAP sub-family.

RESULTS

Thermal stability

Far-UV circular dichroism spectra of rTcMTAP at pH ranging from 4.0 to 9.0, recorded during thermal denaturation, show maximum peak at 192 nm and dichroic bands at 208 and 222 nm (Fig. 1). In addition, the protein spectra pattern, even after the unfolding transition, kept similar to the native, markedly at pH 7.4 and 9.0. To confirm this hypothesis, the secondary structure content was predicted [16] at 20 and 95 °C for all pH (Table 1) using the CDPro software package. The α-helix content showed modest decrease after denaturation, more strikingly at pH 7.4 and 9.0. These data indicate the secondary structure content of rTcMTAP is formed predominantly of α-helix and that thermal denaturation has diminute effect over its content.

The thermal unfolding, which was monitored at 208 nm, appeared as a single transition at pH 4.0, 5.2, 6.0, and 7.4 (Fig. 2) and its data were fitted as a nonlinear extrapolation, according to the van't Hoff approximation [17]. We observed a sigmoid dependence of the ellipticity with the temperature, with practically no alteration until 60 °C, followed by a large change in the ellipticity, which characterized the unfolding

process (Fig. 2). By these results, we assumed that rTcMTAP unfolding process follows a two-state model since the shape of the transition curve is characteristic of a highly cooperative process. The sharp transition curves resulted in melting temperatures (T_m) equal or slightly greater than 79.8 °C (Fig. 2 and Table 2), which were extrapolated from the fitted transition curves. The highest stability at 25 °C (ΔG^{25}) in the absence of additives was at pH 7.4, however its value was very similar to the others pH conditions (Table 2). We also performed thermal denaturation at pH 7.4 in the presence of phosphate, a MTAP substrate, to evaluate its effect on enzyme stability. The ΔG^{25} value almost doubled, from 36 to 61.2 kcal/ mol, when it was added. At pH 4.0, the enzyme showed lower ΔG^{25} when compared to 5.2, 6.0 and 7.4. Although significant differences were observed in ΔG^{25}, T_m values were similar, ranging from 79.8 °C at pH 4.0 to 81.2 °C at pH 7.4.

We also investigated the effect of higher pH over rTcMTAP stability. Although the CD spectra indicated that at pH 9.0 the environment had modest effect over enzyme secondary structure (Fig. 1E, Table 1), the thermal denaturation at pH 8.0, 8.6 and 9.0 exhibited an altered transition slope (Fig. 3). Since the shape of the denaturation slopes were not characteristic of a two-state model transition the thermodynamic parameters could not be calculated for these conditions.

To determine the effects of known protein stabilizers on rTcMTAP, we incubated the enzyme with CTAB or sorbitol at pH 6.0 and 7.4. The thermodynamic parameters were determined (Table 2) and the denaturation curves in the presence (0.1, 0.5 and 1.0 mM) of detergent are shown in Fig. 2 (C and D, respectively). At pH 6.0, CTAB strikingly increased rTcMTAP stability. For instance, in the presence of 0.5 mM CTAB the value of ΔG^{25} triplicate and T_m changed to 97.6 °C. At pH 7.4, CTAB increased the enzyme melting temperature (Table 2), however it became the unfolding reaction less cooperative, as judged by the denaturation curves (Fig. 2D). Unfolding slopes were not observed when the assay was performed in the presence of 1.0 mM of CTAB or sorbitol (0.5 and 1.0 M) at both pHs (data not shown).

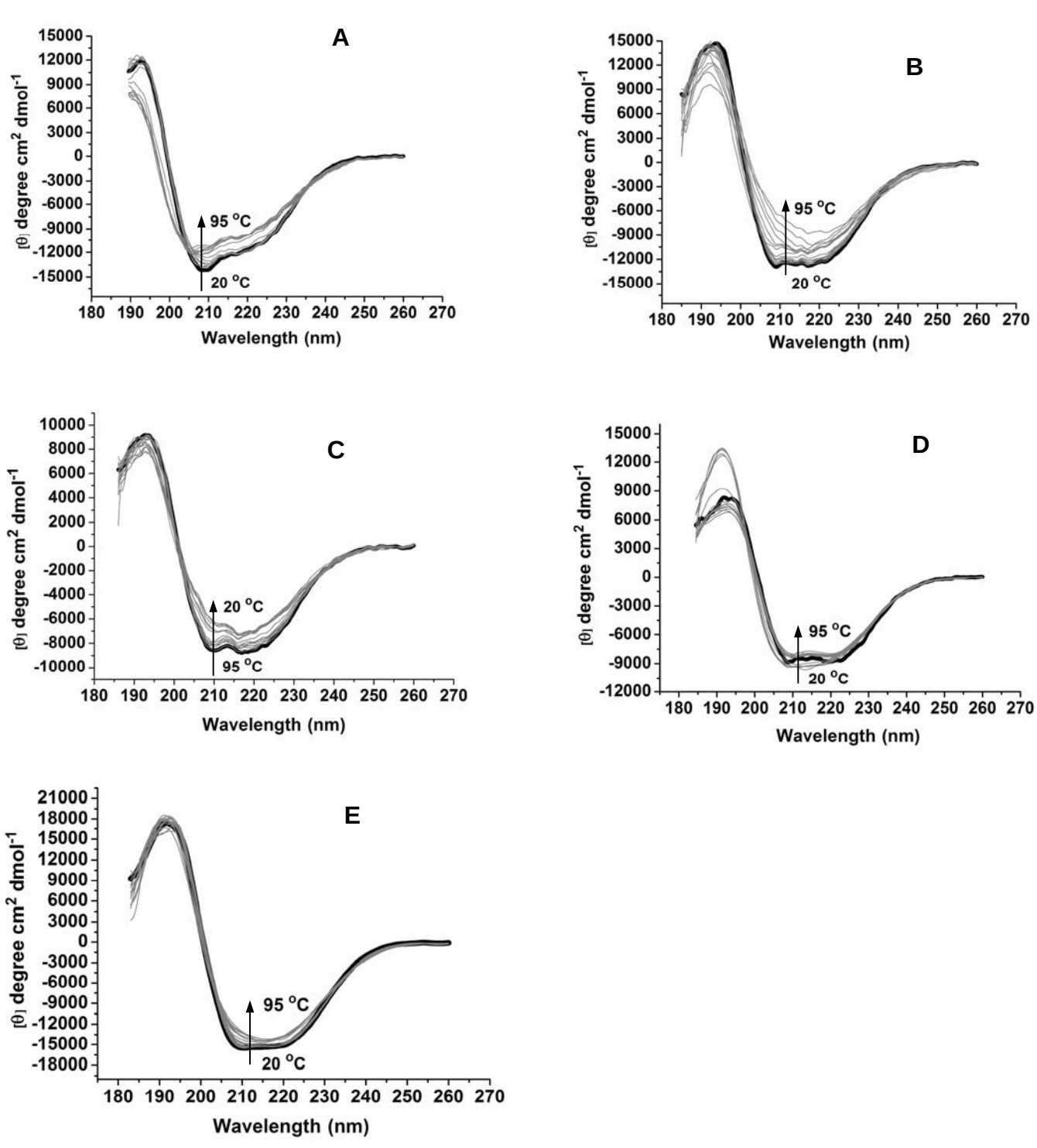

Fig. 1. **rTcMTAP spectra exhibit less variation at higher pH.** Far-UV CD spectra at pH: (A) 4.0; (B) 5.2; (C) 6.0; (D) 7.4; and (E) 9.0 were recorded during thermal denaturation. The bolded spectrum corresponds to 20 °C data.

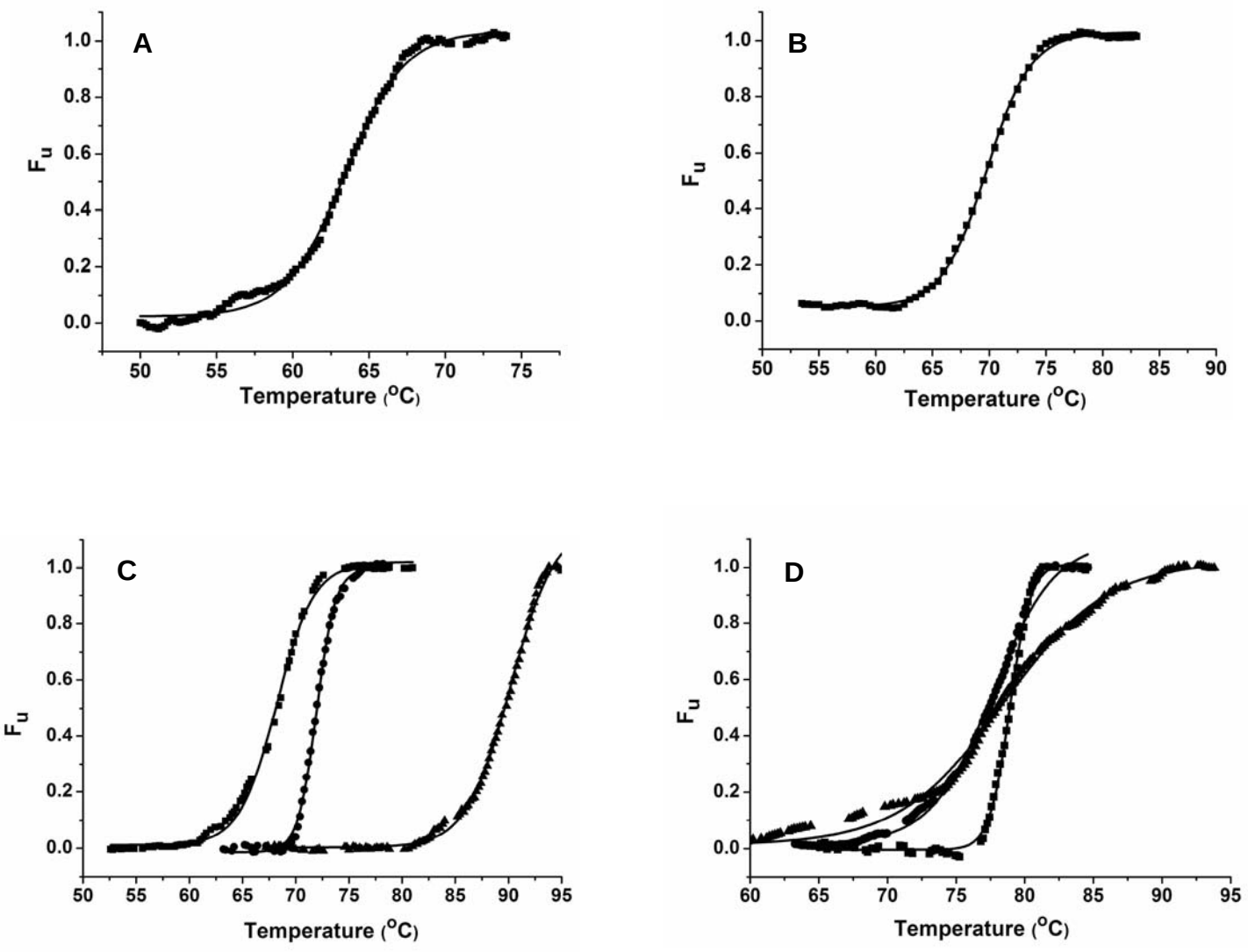

Fig. 2. rTcMTAP resistance to thermal denaturation varies with pH and in the presence of CTAB. Fitted unfolding curves from thermal denaturation data performed at pH: (A) pH 4.0 (B) pH 5.2 (C) pH 6.0 (D) pH 7.4 and in the (■) absence or in the presence of (●) 0.1 mM and (▲) 0.5 mM CTAB. The unfolding process was followed by far-UV CD at 208 nm.

Table 1. Thermal denaturation has discrete effect over rTcMTAP secondary structure content. Each structure content is the average of CDSSTR, CONTINLL and SELCON3 programs estimation for every condition.

pH	Temperature (°C)	α-Helix (%)	β-Sheet (%)	β-Turn (%)	Unordered (%)	Total (%)
4.0	20	37	14	22	28	100
	95	21	24	23	32	100
5.0	20	37	15	20	28	100
	95	22	29	21	28	99
6.0	20	24	25	21	29	99
	95	13	35	23	29	100
7.4	20	26	24	21	29	99
	95	24	24	22	28	99
9.0	20	40	13	20	27	100
	95	36	17	20	27	100

Table 2. CTAB and phosphate influences rTcMTAPthermodynamic parameters. Thermodynamic parameters, melting temperature (T_m), thermal stability at 25 °C (ΔG^{25}), enthalpy (ΔH_u) and entropy (ΔS_u) at unfolding were calculated at different pH in the absence or presence of CTAB.

pH	T_m (ºC)	ΔG^{25} (kcal/ mol)	ΔH_u (kcal/ mol)	ΔS_u (cal/ mol)
4.0	79.8	27.7	180 ± 2	512 ± 6
5.2	80.5	28.9	167 ± 2	465 ± 5
6.0	82.8	32.5	200 ± 3	564 ± 7
6.0 + 0.1 mM CTAB	80.6	47.1	290 ± 1	816 ± 36
6.0 + 0.5 mM CTAB	97.6	112.6	575 ± 8	1553 ± 23
7.4	82.0	36.0	213 ± 3	590 ± 7
7.4 + Phosphate	81.9	61.2	380 ± 6	1071 ± 16
7.4 + 0.1 mM CTAB	98.6	25.3	132 ± 2	360 ± 5
7.4 + 0.5 mM CTAB	118.7	23.5	108 ± 2	284 ± 6

Since the presence of CTAB and sorbitol altered the enzyme stability, we determined if they were also changing the protein structure by recording CD and fluorescence spectra. CTAB red-shifted the fluorescence maximum emission wavelength from 333 to 339 nm and also increased the fluorescence intensity as shown in Fig 4A. However, CTAB at different pH did not induce significant changes in the CD spectra profile (data not shown). In opposite, sorbitol affected the CD spectra, increasing the signal intensity at pH 6.0 (data not shown) and 7.4 (Fig. 4B). However, it did not alter the emission bands position in the fluorescence spectra, although the signal intensity was quenched (Fig. 4C). The linear extrapolation slopes, employed to calculate ΔH_u and ΔS_u, evidenced the CTAB effect over this two parameters (Fig. 5). For instance, at pH 7.4 (Fig. 5, open symbols), CTAB drastically altered the slopes angle, but remained close to each other, reflecting mainly in the alteration of ΔH_u value.(Table 1). At pH 6.0, CTAB increased ΔH_u and ΔS_u values (Table 2), where the ΔS_u change is evidenced by the distance among the slopes (Fig. 5, filled symbols).

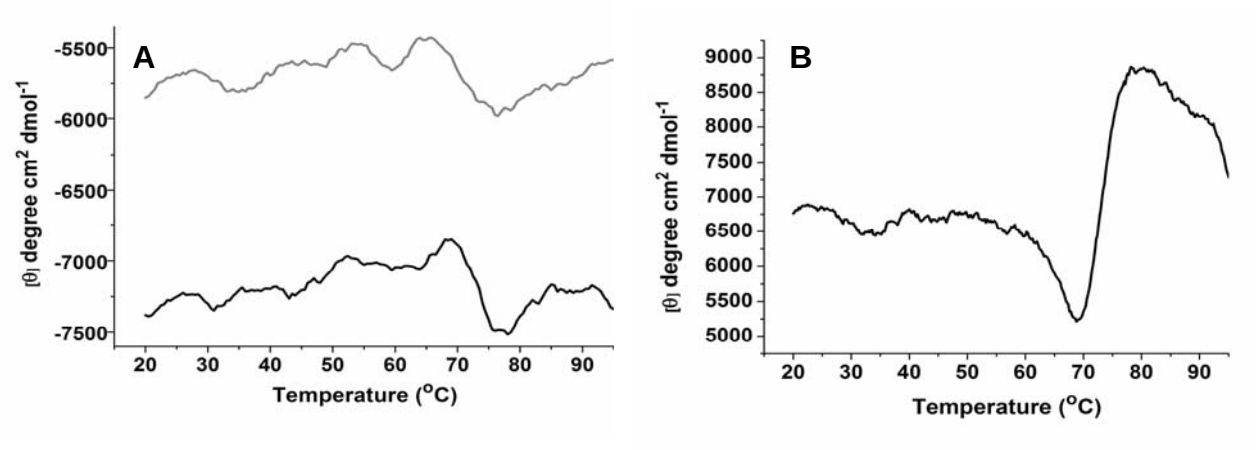

Fig. 3. rTcMTAP transition slope has altered pattern at high pH. Thermal denaturation process exhibited a non-two-state denaturation at pH: (A) 8.0 (gray); 8.6 (black) and (B) 9.0.

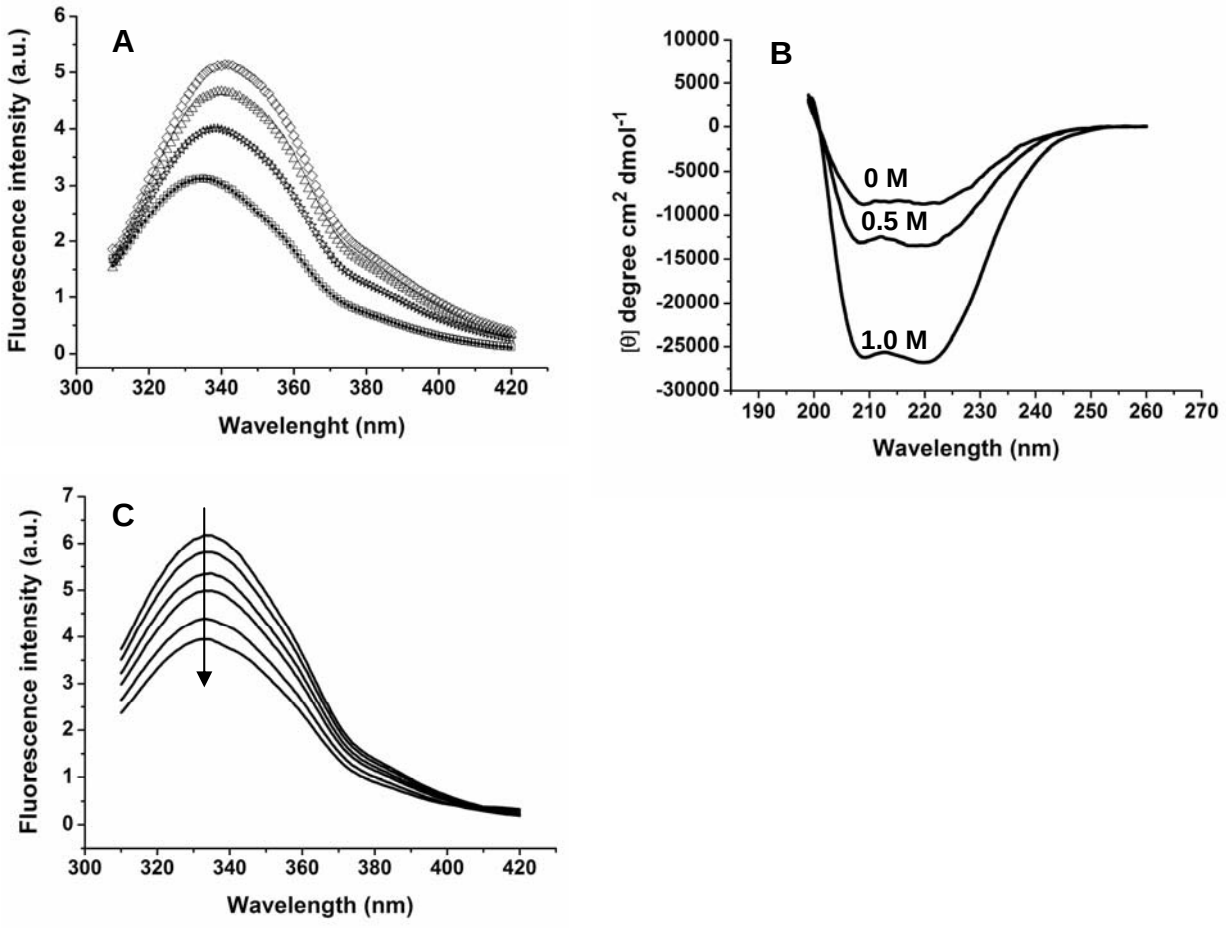

Fig. 4. Stabilizers affect rTcMTAP fluorescence and CD spectra. (A) Fluorescence spectra in the (●) absence or in the presence of (□) 0.1 mM, (☆) 0.5 mM, (△) 1.0 mM and (◊) 2.0 mM CTAB at pH 7.4. (B) CD spectra in the presence of Sorbitol (0 – 1 M). (C) Fluorescence spectra in the presence of Sorbitol: 0 – 1.1 M (bottom).

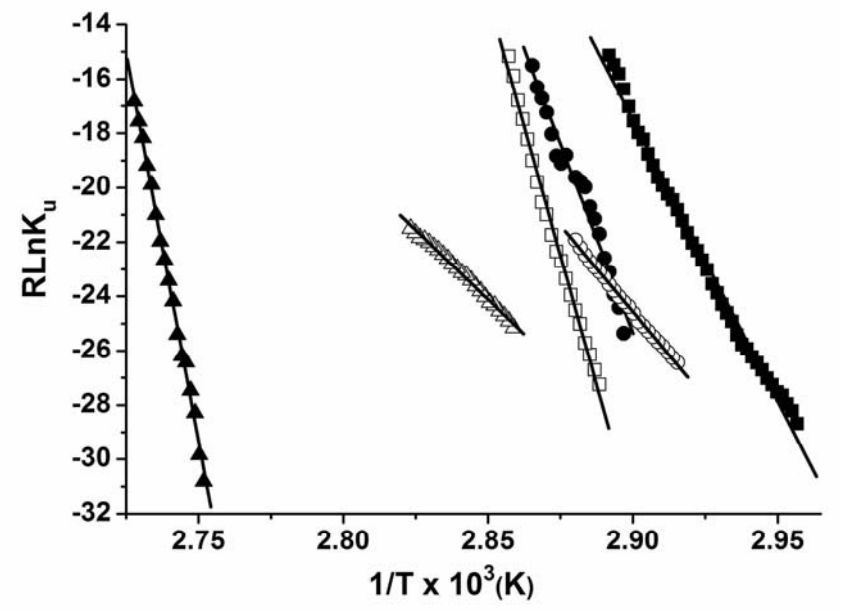

Fig. 5. Comparison of vant't Hoff plot at different pH in absence and presence of CTAB. Data from thermal denaturation at pH 6.0 - filled symbols or pH 7.4 - open symbols in the (■) absence or presence of (●) 0.1 mM, (▲) 0.5 mM CTAB were fitted to van't Hoff expression.

Chemical Equilibrium

Perturbations in the micro-environment of the two tryptophans residues, at positions 167 and 230 of TcMTAP sequence, were evaluated by increasing concentrations of Gnd-HCl and urea followed by fluorescence spectroscopy (Fig. 6). The native rTcMTAP fluorescence spectrum showed a maximum wavelength at 335 nm (Fig. 6 A and B, top spectrum). During Gnd-HCl denaturation, emission spectra positions were preserved with decrease in intensity up to 3.6 M. Thereafter, higher concentrations of Gnd-HCl induced both red-shifting and decreasing in intensity of emission bands. In contrast to the folded state, at 7 M of Gnd-HCl, rTcMTAP emission spectrum adopted maximum wavelength at 352 nm and its intensity dropped to about 45% of that measured for the folded enzyme, characterizing exposure of tryptophans to the solvent. These data suggest that the tryptophans residues are buried in a hydrophobic environment in the folded structure [18] that maintains its native conformation in the presence of Gnd-HCl concentrations as high as 3.6 M. We also recorded rTcMTAP ellipticities at the same experimental conditions. Increasing concentrations of Gnd-HCl induced a sharp unfolding transition curve (Fig. 6C), corroborating the thermal denaturation results (Fig. 2). The stabilization free energy value in absence of Gnd-HCl (ΔG_u^{H2O}) calculated from CD data was 35.5 kcal /mol. In addition to the remarkable resistance to Gnd-HCl, rTcMTAP resisted to urea concentrations as high as 8 M without showing modification in the maximum wavelength band position that could characterize an unfolding process. However, the band intensity decreased in higher concentrations of the urea (Fig. 6B). Likewise the fluorescence assay, the CD ellipticities in the presence of urea did not exhibit a transition pattern (data not shown).

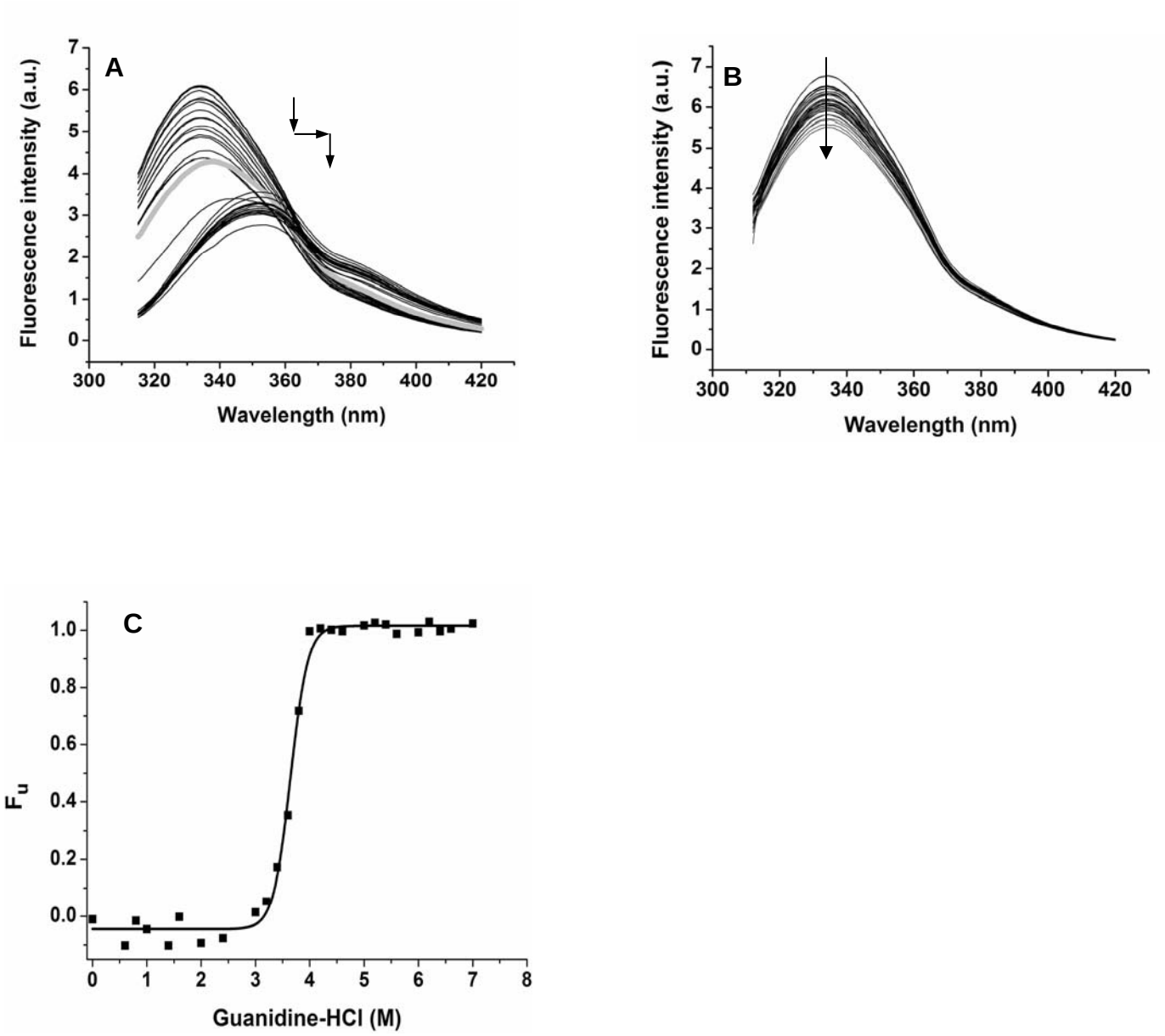

Fig. 6. rTcMTAP keep folded until 3.6 M Gnd-HCl or 8 M urea. Fluorescence emission spectra of rTcMTAP in presence of: (A) Gnd-HCl (0 – 7 M), gray spectrum represents 3.8 M. (B) urea (0 – 8 M). (C) Fitted Gnd-HCl-induced unfolding curve followed by CD. The arrows indicate the maximum wavelength path throughout the assay.

DISCUSSION

Equilibrium denaturation studies on the folding/unfolding of proteins have largely been done on small monomeric globular proteins. Nevertheless, analysis of the forces and energies involved in the folding and packing of oligomeric proteins could provide additional information on subunit interactions and in the folding process [7-9,19,20]. The main difference between mono and oligomeric folding is the existence of interactions between the protein subunits. Consequently, the intra and intermolecular interactions of the folding pathway must be taken into account since it will influence the overall stability and integrity of oligomeric proteins.

TcMTAP has been characterized as a dimer [21] and our previous work [14] showed that rTcMTAP subunits association is probably kept by weak interactions. Besides that, data from dynamic light scattering corroborate that rTcMTAP associate into oligomeric species (data not shown). It has been shown that some proteins assemble into dimers through weak interations, but still present a two-state denaturation. In this case, the thermodynamic stability comes from the stabilization of each monomer [22,23]. Sigmoidal curves, characteristic of cooperative unfolding transitions, were obtained for rTcMTAP under chemical and thermal denaturation conditions, accompanied by CD and fluorescence spectroscopy. These data indicate that the dimer structural arrangement of rTcMTAP denatures in a two-state pathway because no alteration on spectra prior the transition was detected.

Thus, the analysis of denaturation curves in this study was based on the assumption that only the folded and the unfolded forms of rTcMTAP exist at equilibrium. This assumption is based on that dimer dissociation leads to the formation of an intrinsically unstable species, hence folded monomeric species will not significantly populate at equilibrium. Although dimeric proteins have additional modes of quaternary structure stabilization, many still follow a two-state transition [9,24].

The values of thermodynamic parameters indicate that rTcMTAP exhibits considerable stability at acid and neutral pH, but not at basic pH. This correlates well to the activity of rTcMTAP in a broad pH range, expect at pH 8.6 or higher [14]. The lower activity at basic pH might be correlated the altered transition curves observed at these conditions. The CD signal fluctuation observed prior to 70 °C at over-7.4 pH is probably due to ionization effect altering the intramolecular and intermolecular interactions associated with the catalytic sites.

A possible evolutionary explanation to rTcMTAP thermal resistance is the primary sequence identity with MTAPs from thermophilic organisms [14]. rTcMTAP highest stability in the absence of stabilizers CTAB and sorbitol was observed at pH 7.4 with phosphate. This result indicates that the binding of this substrate raises the conformational stability of the enzyme, thus reducing its susceptibility to thermal denaturation. Phosphate induced similar protection in MTAP from *Sulfolobus solfataricus* and *Pyrococcus furiosus* [25,26]. In contrast, the lowest ΔG^{25} was obtained at pH 4.0 which may reflect that lower pH cause disruption of critical interactions upon protonation, thus decreasing protein stability [27].

Sorbitol, a polyol, probably increased rTcMTAP stability, but the thermodynamic parameters were impossible to calculate because the slopes of thermal denaturarion did not exhibit an evident unfolding pattern. Although sorbitol increased the CD signal, it did not alter the shape of the spectra which we suppose to reflect alterations in protein compactness or oligomerization state. Some sugars and polyols have been found to raise protein's denaturation temperature by as much as 15 °C [28]. The most common explanation to sorbitol's protective effect is that this osmolyte raises the surface tension of the medium, which leads to a preferential hydration of the protein, resulting in a decreased hydrogen-bond rupturing capacity of the medium [29-31]. In contrast, CTAB, a cationic surfactant, increased protein's ΔG^{25} but did not avoid rTcMTAP thermal denaturation. The high stability at pH 6.0 was mostly entropy-driven, reflecting an improved organization of environment molecules with rTcMTAP. In opposite, the reduced stability induced by CTAB at pH 7.4 was enthalpy-driven, indicationg rupture of enzyme intramolecular bonds. CTAB at concentration below its critical micelle concentration (c.m.c = 1.1 mM) seems to interact with apolar parts through introducing its hydrophobic chain inside hydrophobic cavities of the protein [32]. We observed that CTAB at pH 7.4 has a negative influence on enzyme stability, probably because it perturbs, what seems to be, the best configuration of non-covalent interactions that rTcMTAP establishes. CTAB also induced both increasing and red-shifting of rTcMTAP fluorescence indicating that Trp residues are more exposed to polar environment. The increased intensity of fluorescence suggests that the exposure of Trp167 led to disruption of the internal quenching effect of Arg168 in the native conformation, which is a known quenching circumstance [33].

The enzyme exhibited remarkable resistance to chemical denaturation keeping folded in concentrations as high as 3.6 M of Gnd-HCl and 8 M. The decreased intensity

of fluorescence prior to 3.6 M Gnd-HCl and in the urea assay is the quenching effect caused by higher concentration of the denaturant. Comparing the $\Delta G_u(H_2O)$ from CD data (35.5 Kcal/mol) and the ΔG^{25} from thermal denaturation we observe a good concordance between the results from CD indicating that this technique is likely to reflect the full unfolding process of rTcMTAP. Since results from thermal and chemical denaturation were coincident corroborates the assumption that rTcMTAP unfolds in a two-way fashion. To confirm this supposition we suggest that different approaches should be used, e. g. fluorescence and CD in different protein concentrations and conditions, nuclear magnetic resonance, in addition to activity measurements and differential scanning calorimetry (DSC). In addition, Neet [9], suggested a relationship between the size of the dimer and the protein structure stabilization, since a linear correlation was observed between the number of amino acid residues (N) in the monomer and the value of $\Delta G_u^{H2O} = 8.8 + 0.08N$ kcal/mol. The formula-predicted $\Delta G_u(H_2O)$ is 35.2 kcal/mol, a close estimative to that experimentally obtained, again corroborating the results from CD data.

In this work we characterized thermodynamically the recombinant methylthioadenosine phosphorylase of *T. cruzi*. The enzyme exhibits remarkable chemical and thermal resistance; the latter was increased in presence of stabilizer sorbitol and CTAB. The highest stability was achieved at pH 7.4 in the presence of phosphate, corroborating the protection role played by this substrate. However, the tested additives seem to alter the enzyme's secondary and tertiary structure. We also observed that rTcMTAP unfolds in a two-state model.

MATERIALS AND METHODS

Recombinant protein production and purification

Recombinant TcMTAP was heterologously produced in *E. coli* BL21-DE3 strain and purified as described [14]. Enzyme stock used in our experiments was not more than 1 week old. The protein purity was determined by SDS-PAGE and concentration was monitored by measuring the absorbance at 280 nm using the extinction coefficient of 21980 $M^{-1}.cm^{-1}$, calculated using the Protparam tool (http://www.expasy.org/tools/protparam.html).

Circular dichroism spectroscopy

Circular dichroism measurements were carried out on a JASCO J-810 spectropolarimeter equipped with a Peltier-type temperature controller and a thermostated cell holder interfaced with a thermostatic bath. Far-UV spectra (185 to 260 nm) were recorded in 0.1-cm pathlength quartz cells at a protein concentration of 0.1 mg/mL (3.0 μM) in 2.5 mM buffers: Na-acetate pH 4.0, Sodium-acetate pH 5.2; bis-Tris pH 6.0, Potassium-phosphate pH 7.4, or Tris-HCl pH 9.0. Spectra from pH 6.0 and 7.4 in the presence of CTAB (0.1, 0.5 and 1.0 mM) or sorbitol (0.5 and 1.0 M) were also collected. To determine the thermodynamic parameters we performed thermal denaturation at the above pH and also at Tris-HCl pH 7.4, 8.0 and 8.6. The spectra presented in this work represent the average of four accumulated consecutive scans. Thermal denaturation assays were performed by increasing the temperature from 20 to 95 °C, allowing the temperature stabilization for 5 min before recording each spectrum. The data were corrected for the baseline contribution of the buffer and the observed ellipticities at 208 nm were recorded. The ellipticities were converted into the mean residue ellipticities [θ] based on the mean molecular mass residue of rTcMTAP. Data were analyzed by assuming a two-state transition considering the changes in the [θ]. The overall unfolding reaction starts with the folded dimer (A_2) and end with two unfolded monomers (2U). The overall reaction may be described by the following:

$$A_2 \overset{K_U}{\leftrightarrow} 2U$$

Where, $K_U = [U]^2 / [A_2] = 4 f_d^2 P_t / (1- f_d)$ and $\Delta G_u = -RT \text{ Ln } K_u$

K_u is the dissociation constant, f_d is the molar fraction of denatured protein, P_t is the total protein molar concentration (monomers unit). Evaluation of K_u and extrapolation to standard conditions to obtain Gibbs free energy (ΔG_u) can be performed as for monomeric proteins. Thermodynamic parameters derived from the transition curves were calculated by linear extrapolation method (LEM).

Secondary structure content was estimated from far-UV CD spectra using the SELCON3, CDSSTR and CONTINLL software, from CDPro suite (http://lamar.colostate.edu/~sreeram/CDPro). It was employed the reference set of 50 proteins, SMP50. Showed contents are an average of the three programs results.

Isothermal Guanidine hydrochloride-induced Denaturation

Equilibrium unfolding as function of guanidine hydrochloride (Gnd-HCl) concentration was monitored by fluorescence spectroscopy and circular dichroism. Each sample of rTcMTAP, 0.1 mg/ mL in 10 mM potassium phosphate buffer pH 7.4, was incubated in the presence of 0-7 M Gnd-HCl or 0-8 M urea, both at 0.2 M intervals, and equilibrated for 24 h prior measurements. Fluorescence measurements were carried on an Aminco Bowman Series 2 (SLM Aminco) luminescence spectrometer using a 1 × 1 cm path length cuvette with water-jacketed cell previously stabilized at 25 °C in all experiments. Excitation wavelength was at 280 nm and the emission was recorded from 310 to 420 nm with 1 nm increment. The CD data were collected by the same apparatus used in circular dichroism assay. Each condition spectra were corrected subtracting the signal of the buffer different denaturant concentrations.

REFERENCES

[1] Avila MA, Garcia-Trevijano ER, Lu SC, Corrales FJ & Mato JM (2004). Methylthioadenosine. *Int J Biochem Cell Biol* **36**, 2125-2130.

[2] Pollock PM, Pearson JV & Hayward NK (1996). Compilation of somatic mutations of the CDKN2 gene in human cancers: non-random distribution of base substitutions. *Genes Chromosomes Cancer* **15**, 77-88.

[3] Smith-Sorensen B & Hovig E (1996). CDKN2A (p16INK4A) somatic and germline mutations. *Hum Mutat* **7**, 294-303.

[4] Ghoda LY, Savarese TM, Northup CH, Parks RE, Jr., Garofalo J, Katz L, Ellenbogen BB & Bacchi CJ (1988). Substrate specificities of 5'-deoxy-5'-methylthioadenosine phosphorylase from Trypanosoma brucei brucei and mammalian cells. *Mol Biochem Parasitol* **27**, 109-118.

[5] Bacchi CJ, Sufrin JR, Nathan HC, Spiess AJ, Hannan T, Garofalo J, Alecia K, Katz L & Yarlett N (1991). 5'-Alkyl-substituted analogs of 5'-methylthioadenosine as trypanocides. *Antimicrob Agents Chemother* **35**, 1315-1320.

[6] Bacchi CJ, Sanabria K, Spiess AJ, Vargas M, Marasco CJ, Jr., Jimenez LM, Goldberg B & Sufrin JR (1997). In vivo efficacies of 5'-methylthioadenosine analogs as trypanocides. *Antimicrob Agents Chemother* **41**, 2108-2112.

[7] Sacchetta P, Aceto A, Bucciarelli T, Dragani B, Santarone S, Allocati N & Di Ilio C (1993). Multiphasic denaturation of glutathione transferase B1-1 by guanidinium chloride. Role of the dimeric structure on the flexibility of the active site. *Eur J Biochem* **215**, 741-745.

[8] Brandau DT, Jones LS, Wiethoff CM, Rexroad J & Middaugh CR (2003). Thermal stability of vaccines. *J Pharm Sci* **92**, 218-231.

[9] Neet KE & Timm DE (1994). Conformational stability of dimeric proteins: quantitative studies by equilibrium denaturation. *Protein Sci* **3**, 2167-2174.

[10] Holdgate GA & Ward WH (2005). Measurements of binding thermodynamics in drug discovery. *Drug Discov Today* **10**, 1543-1550.

[11] Urbina JA (2001). Specific treatment of Chagas disease: current status and new developments. *Curr Opin Infect Dis* **14**, 733-741.

[12] Bacchi CJ, Goldberg B, Rattendi D, Gorrell TE, Spiess AJ & Sufrin JR (1999). Metabolic effects of a methylthioadenosine phosphorylase substrate analog on African trypanosomes. *Biochem Pharmacol* **57**, 89-96.

[13] Berens RL KE, Marr JJ (1995) in: *Biochemistry and molecular biology of parasites.*, pp. 89-117 (M, M.J.a.M., Ed.) Academic Press, London.

[14] Neves D, Bastos ID, de Lima MM, Restrepo-Cadavid G, Teixeira ARL, Medrano FJ, Grellier P, Schrevel J, Campbell DA & Santana JM (2006). The Methylthioadenosine phosphorylase of *Trypanosoma cruzi* is mesophilic and displays broad substrate specificity.

[15] Wielgus-Kutrowska B, Bzowska A, Tebbe J, Koellner G & Shugar D (2002). Purine nucleoside phosphorylase from Cellulomonas sp.: physicochemical properties and binding of substrates determined by ligand-dependent enhancement of enzyme intrinsic fluorescence, and by protective effects of ligands on thermal inactivation of the enzyme. *Biochim Biophys Acta* **1597**, 320-334.

[16] Bolotina IA (1987). [Secondary structure of proteins from circular dichroism spectra. V. Secondary structure of proteins in a "molten globule" state]. *Mol Biol (Mosk)* **21**, 1625-1635.

[17] Santoro MM & Bolen DW (1992). A test of the linear extrapolation of unfolding free energy changes over an extended denaturant concentration range. *Biochemistry* **31**, 4901-4907.

[18] Teale FW (1960). The ultraviolet fluorescence of proteins in neutral solution. *Biochem J* **76**, 381-388.

[19] Timm DE, de Haseth PL & Neet KE (1994). Comparative equilibrium denaturation studies of the neurotrophins: nerve growth factor, brain-derived neurotrophic factor, neurotrophin 3, and neurotrophin 4/5. *Biochemistry* **33**, 4667-4676.

[20] Wallace LA, Sluis-Cremer N & Dirr HW (1998). Equilibrium and kinetic unfolding properties of dimeric human glutathione transferase A1-1. *Biochemistry* **37**, 5320-5328.

[21] Miller RL, Sabourin CL & Krenitsky TA (1987). Trypanosoma cruzi adenine nucleoside phosphorylase. Purification and substrate specificity. *Biochem Pharmacol* **36**, 553-560.

[22] Cunningham BC, Mulkerrin MG & Wells JA (1991). Dimerization of human growth hormone by zinc. *Science* **253**, 545-548.

[23] Pace NC & Tanford C (1968). Thermodynamics of the unfolding of beta-lactoglobulin A in aqueous urea solutions between 5 and 55 degrees. *Biochemistry* **7**, 198-208.

[24] Ahmad N, Srinivas VR, Reddy GB & Surolia A (1998). Thermodynamic characterization of the conformational stability of the homodimeric protein, pea lectin. *Biochemistry* **37**, 16765-16772.

[25] Cacciapuoti G, Forte S, Moretti MA, Brio A, Zappia V & Porcelli M (2005). A novel hyperthermostable 5'-deoxy-5'-methylthioadenosine phosphorylase from the archaeon Sulfolobus solfataricus. *Febs J* **272**, 1886-1899.

[26] Cacciapuoti G, Bertoldo C, Brio A, Zappia V & Porcelli M (2003). Purification and characterization of 5'-methylthioadenosine phosphorylase from the hyperthermophilic archaeon Pyrococcus furiosus: substrate specificity and primary structure analysis. *Extremophiles* **7**, 159-168.

[27] Hughson FM & Baldwin RL (1989). Use of site-directed mutagenesis to destabilize native apomyoglobin relative to folding intermediates. *Biochemistry* **28**, 4415-4422.

[28] Back JF, Oakenfull D & Smith MB (1979). Increased thermal stability of proteins in the presence of sugars and polyols. *Biochemistry* **18**, 5191-5196.

[29] Gerlsma S (1968). Reversible denaturation of ribonuclease in aqueous solutions as influenced by polyhydric alcohols and some other additives. *The Journal of biological chemistry* **243**, 957-961.

[30] Gerlsma SY (1970). The effects of polyhydric and monohydric alcohols on the heat induced reversible denaturation of chymotrypsinogen A. *Eur J Biochem* **14**, 150-153.

[31] Tiwari A & Bhat R (2006). Stabilization of yeast hexokinase A by polyol osmolytes: Correlation with the physicochemical properties of aqueous solutions. *Biophys Chem*.

[32] Liu W, Guo X & Guo R (2005). The interaction of hemoglobin with hexadecyltrimethylammonium bromide. *Int J Biol Macromol* **37**, 232-238.

[33] Permyakov E (1993) CRC Press, Boca Raton, FL, USA.

CONCLUSÕES

CONCLUSÕES

Este trabalho teve como objetivo caracterizar molecular, bioquímica e biofisicamente a enzima metiltioadenosina fosforilase do parasita *Trypanosoma cruzi*, agente etiológico da doença de Chagas. Os dados obtidos permitem as seguintes conclusões:

O gene que codifica a TcMTAP (*Tcmtap*) está representado por uma única cópia por genoma haplóide do *T. cruzi;*

O *Tcmtap* tem uma fase aberta de leitura de 921 pares de base que codifica uma proteína da família 2 das fosforilases de nucleosídeos purínicos;

A TcMTAP é diferencialmente expressa pelas diferentes formas de *T. cruzi* e sua forma recombinante produzida em bactéria organiniza-se em estrutura oligomérica;

Diferente de sua homóloga humana que é altamente específica para MTA, a TcMTAP apresenta ampla especificidade para substratos;

Apesar de ser ativa em ampla faixa de pH e temperatura, a TcMTAP tem atividade ótima em pH 7,4 e 50 °C;

A TcMTAP é altamente resistente à desnaturação térmica e química e apresenta desnaturação em dois estágios.

A estabilidade da enzima tem pouca dependência das condições ionizantes do ambiente;

As diferenças bioquímicas e cinéticas com a MTAP humana sugerem que a TcMTAP pode ser explorada como alvo de drogas que poderiam vir a ser utilizadas como fármacos para quimioterapia da doença de Chagas. Características biofísicas melhoram nosso conhecimento sobre o comportamento da TcMTAP em diferentes ambientes, fornecendo condições para o desenvolvimento racional de inibidores específicos.

Outra vertente que já está sendo explorada por nosso grupo é a determinação da estrutura tridimensional da molécula a partir de difração de raios-X. A elucidação da estrutura, a partir da identificação de características exclusivas em comparação à enzima do hospedeiro mamífero, permitirá a síntese racional de inibidores altamente específicos. Além disso, os estados de transição da reação enzimática e o estado oligomérico da proteína poderão ser determinados. Nós já obtivemos cristais da proteína, contudo estavam em tamanho insuficiente para determinar seus parâmetros ou a coleta dos dados. Em breve as condições de cristalização serão refinadas para obtenção de melhores cristais e consequentemente coleta dos dados para resolução final.

PERSPECTIVAS

PERSPECTIVAS

Dando prosseguimento ao nosso trabalho que tem como principais objetivos obter dados sobre função e estrutura da TcMTAP e o desenho racional de inibidores específicos, nós procederemos à neutralizção do *Tcmtap* por meio de recombinação genética, seguida de caracterização dos mutantes. Concomitantemente, faremos a resolução da estrutura tridimensional da rTcMTAP que permitirá desenhar inibidores e varrer bibliotecas virtuais de possíveis inibidores. Neste contexto, as diferenças entre as estruturas da TcMTAP e hMTAP serão consideradas no sentido de obtenção de inibidores específicos. Após testes *in vitro*, os melhores inibidores serão testados *in vivo*.

BIBLIOGRAFIA

BIBLIOGRAFIA

Agarwal, K. C. and Parks, R. E., Jr. (1972). Adenosine triphosphate-guanosine 5'-phosphate phosphotransferase. IV. Isozymes in human erythrocytes and Sarcoma 180 ascites cells. **Mol Pharmacol** 8(2): 128-38.

Bacchi, C. J., Garofalo, J., Mockenhaupt, D., McCann, P. P., Diekema, K. A., Pegg, A. E., Nathan, H. C., Mullaney, E. A., Chunosoff, L., Sjoerdsma, A. and Hutner, S. H. (1983). In vivo effects of alpha-DL-difluoromethylornithine on the metabolism and morphology of Trypanosoma brucei brucei. **Mol Biochem Parasitol** 7(3): 209-25.

Bacchi, C. J., Nathan, H. C., Clarkson, A. B., Jr., Bienen, E. J., Bitonti, A. J., McCann, P. P. and Sjoerdsma, A. (1987). Effects of the ornithine decarboxylase inhibitors DL-alpha-difluoromethylornithine and alpha-monofluoromethyldehydroornithine methyl ester alone and in combination with suramin against Trypanosoma brucei brucei central nervous system models. **Am J Trop Med Hyg** 36(1): 46-52.

Bacchi, C. J., Sanabria, K., Spiess, A. J., Vargas, M., Marasco, C. J., Jr., Jimenez, L. M., Goldberg, B. and Sufrin, J. R. (1997). In vivo efficacies of 5'-methylthioadenosine analogs as trypanocides. **Antimicrob Agents Chemother** 41(10): 2108-12.

Batova, A., Diccianni, M. B., Omura-Minamisawa, M., Yu, J., Carrera, C. J., Bridgeman, L. J., Kung, F. H., Pullen, J., Amylon, M. D. and Yu, A. L. (1999). Use of Alanosine as a Methylthioadenosine Phosphorylase-Selective Therapy for T-Cell Acute Lymphoblastic Leukemia in Vitro. **Cancer Research** 59: 1492 - 7.

Behrmann, I., Wallner, S., Komyod, W., Heinrich, P. C., Schuierer, M., Buettner, R. and Bosserhoff, A. K. (2003). Characterization of methylthioadenosin phosphorylase (MTAP) expression in malignant melanoma. **Am J Pathol** 163(2): 683-90.

Brat, D. J., James, C. D., Jedlicka, A. E., Connolly, D. C., Chang, E., Castellani, R. J., Schmid, M., Schiller, M., Carson, D. A. and Burger, P. C. (1999). Molecular genetic alterations in radiation-induced astrocytomas. **Am J Pathol** 154(5): 1431-8.

Brener, Z. (1972). A new aspect of Trypanosoma cruzi life-cycle in the invertebrate host. **J Protozool** 19(1): 23-7.

Brener, Z., Andrade, Z. A. and Barral, M. N. (2000). **Trypanossoma cruzi e Doença de Chagas.** Rio de Janeiro, Editora Guanabara.

Burns, C. L., St Clair, M. H., Frick, L. W., Spector, T., Averett, D. R., English, M. L., Holmes, T. J., Krenitsky, T. A. and Koszalka, G. W. (1993). Novel 6-alkoxypurine 2',3'-dideoxynucleosides as inhibitors of the cytopathic effect of the human immunodeficiency virus. **J Med Chem** 36(3): 378-84.

Burstein, E. A. (1976). **Luminescence of Protein Chromophores (Model Studies)**. Moscow, VINITI.

Burstein, E. A. (1977). **Intrinsic Protein Luminescence (Origins and Applications)**. Moscow, VINITI.

Buxton, R. S., Hammer-Jespersen, K. and Valentin-Hansen, P. (1980). A second purine nucleoside phosphorylase in Escherichia coli K-12. I. Xanthosine phosphorylase regulatory mutants isolated as secondary-site revertants of a deoD mutant. **Mol Gen Genet** 179(2): 331-40.

Bzowska, A., Kulikowska, E. and Shugar, D. (2000). Purine nucleoside phosphorylases: properties, functions, and clinical aspects. **Pharmacol Ther** 88(3): 349-425.

Bzowska, A., Tebbe, J., Luic, M., Wielgus-Kutrowska, B., Schroder, W., Shugar, D., Saenger, W. and Koellner, G. (1998). Crystallization and preliminary X-ray studies of purine nucleoside phosphorylase from Cellulomonas sp. **Acta Crystallogr D Biol Crystallogr** 54(Pt 5): 1061-3.

Cacciapuoti, G., Porcelli, M., Bertoldo, C., De Rosa, M. and Zappia, V. (1994). Purification and characterization of extremely thermophilic and thermostable 5'-methylthioadenosine phosphorylase from the archaeon Sulfolobus solfataricus. Purine nucleoside phosphorylase activity and evidence for intersubunit disulfide bonds. **J Biol Chem** 269(40): 24762-9.

Chae, W.-G., Chan, D. C. K. and Chang, C. (1998). Facile synthesis of 5'-deoxy- and 2',5'-dideoxy-6-thiopurine nucleosides by nucleoside phosphorylases. **Tetrahedron** 54: 8661-70.

Chagas, C. (1909). Nova Tripanosomíase Humana. Estudos sobre a morfologia e o ciclo evolutivo do Schizotrypanum cruzi n.gen.,n. sp., agente etiológico de nova entidade mórbida do homem. **Mem. Inst. Oswaldo Cruz** 1: 159 - 218.

Christopher, S. A., Diegelman, P., Porter, C. W. and Kruger, W. D. (2002). Methylthioadenosine phosphorylase, a gene frequently codeleted with p16(cdkN2a/ARF), acts as a tumor suppressor in a breast cancer cell line. **Cancer Res** 62(22): 6639-44.

Cohen, S. S. (1998). **A guide to the Polyamines**. Oxford, UK, Oxford University Press.

Colucci, W. J., Tilstra, L., Sattler, M. C., Fronczek, F. R. and Barkley, M. D. (1990). Conformational studies of a constained tryptophan derivative: Implications for the fluorescence quenching mechanism. **J. Am. Chem. Soc.** 112: 9182-90.

Deghaide, N. H., Dantas, R. O. and Donadi, E. A. (1998). HLA class I and II profiles of patients presenting with Chagas' disease. **Dig Dis Sci** 43(2): 246-52.

Della Ragione, F., Takabayashi, K., Mastropietro, S., Mercurio, C., Oliva, A., Russo, G. L., Della Pietra, V., Borriello, A., Nobori, T., Carson, D. A. and Zappia, V. (1996). Purification and characterization of recombinant human 5'-methylthioadenosine phosphorylase: definite identification of coding cDNA. **Biochem Biophys Res Commun** 223(3): 514-9.

Duan, D. S., Nagashima, T., Hoshino, T., Waldman, F., Pawlak, K. and Sadee, W. (1990). Mechanisms of 2'-deoxyguanosine toxicity in mouse T-lymphoma cells with purine nucleoside phosphorylase deficiency and resistance to inhibition of ribonucleotide reductase by dGTP. **Biochem J** 268: 725 - 31.

Ealick, S. E., Rule, S. A., Carter, D. C., Greenhough, T. J., Babu, Y. S., Cook, W. J., Habash, J., Helliwell, J. R., Stoeckler, J. D., Parks, R. E., Jr. and et al. (1990). Three-dimensional structure of human erythrocytic purine nucleoside phosphorylase at 3.2 A resolution. **J Biol Chem** 265(3): 1812-20.

Eftink, M. R. (1994). The use of fluorescence methods to monitor unfolding transitions in proteins. **Biophys J** 66(2 Pt 1): 482-501.

Eftink, M. R. and Shastry, M. C. (1997). Fluorescence methods for studying kinetics of protein-folding reactions. **Methods Enzymol** 278: 258-86.

el Kouni, M. H. (2003). Potential chemotherapeutic targets in the purine metabolism of parasites. **Pharmacol Ther** 99(3): 283-309.

ElMunzer, B. J., Sallach, S. M. and McGuire, D. K. (2004). Cardiac chagas disease masquerading as an acute myocardial infarction. **Cardiol Rev** 12(2): 69-72.

Erion, M. D., Stoeckler, J. D., Guida, W. C., Walter, R. L. and Ealick, S. E. (1997). Purine nucleoside phosphorylase. 2. Catalytic mechanism. **Biochemistry** 36(39): 11735-48.

Fish, W. R., Marr, J. J. and Berens, R. L. (1982). Purine metabolism in Trypanosoma brucei gambiense. **Biochim Biophys Acta** 714(3): 422-8.

Friedkin, M. (1950). Deoxyriboside-1-phosphate: II. The isolation of the crystalline deoxyribose-1-phosphate. **J Biol Chem** 184: 449 - 59.

Ghoda, L. Y., Savarese, T. M., Northup, C. H., Parks, R. E., Jr., Garofalo, J., Katz, L., Ellenbogen, B. B. and Bacchi, C. J. (1988). Substrate specificities of 5'-deoxy-5'-methylthioadenosine phosphorylase from Trypanosoma brucei brucei and mammalian cells. **Mol Biochem Parasitol** 27(2-3): 109-18.

Giblett, E. R., Ammann, A. J., Wara, D. W., Sandman, R. and Diamond, L. K. (1975). Nucleoside-phosphorylase deficiency in a child with severely defective T-cell immunity and normal B-cell immunity. **Lancet** 1(7914): 1010-3.

Gilbertsen, R. B. and Sircar, J. C. (1990). Enzyme cascades: purine metabolism and immunosuppression. Comprehensive Medicinal Chemistry. C. Hansch, P.G., S. and Taylor, J. B. Oxford, Pergamon. **2:** 443 - 80.

Haemmerli, S. D., Suleiman, A. A. and Guilbault, G. G. (1990). Amperometric determination of phosphate by use of a nucleoside phosphorylase-xanthine oxidase enzyme sensor based on a Clark-type hydrogen peroxide or oxygen electrode. **Anal Biochem** 191(1): 106-9.

Hamamoto, T., Noguchi, T. and Midorikawa, Y. (1996). Purification and characterization of purine nucleoside phosphorylase and pyrimidine nucleoside phosphorylase from Bacillus stearothermophilus TH 6-2. **Biosci Biotechnol Biochem** 60(7): 1179-80.

Hershfield, M. S. and Mitchell, B. S. (1995). Immunodeficiency diseases caused by adenosine deaminase deficiency and purine nucleoside phosphorylase deficiency. The metabolic and molecular bases of inherited disease. C. R. Scriver, Beaudet, A. L., Sly, W. S. and Valle, D. New York, McGraw-Hill**:** 1725 - 68.

Hori, N., Watanabe, M., Yamazaki, Y. and Mikami, Y. (1989a). Purification and characterization of second thermostable purine nucleoside phosphorylase of *Bacillus stearothermophilus* JTS 859. **Agric Biol Chem** 53: 3219 - 24.

Hori, N., Watanabe, M., Yamazaki, Y. and Mikami, Y. (1989b). Purification and characterization of thermostable purine nucleoside phosphorylase of *Bacillus stearothermophilus* JTS 859. **Agric Biol Chem** 53: 2205 - 10.

Jackson, S. E. and Fersht, A. R. (1991). Folding of chymotrypsin inhibitor 2. 1. Evidence for a two-state transition. **Biochemistry** 30(43): 10428-35.

Jensen, K. F. and Nygaard, P. (1975). Purine nucleoside phosphorylase from Escherichia coli and Salmonella typhimurium. Purification and some properties. **Eur J Biochem** 51(1): 253-65.

Koszalka, G. W. and Krenitsky, T. A. (1986). 5'-Methylthioadenosine (MTA) phosphorylase from promastigotes of Leishmania donovani. **Adv Exp Med Biol** 195 Pt B: 559-63.

Krenitsky, T. A., Koszalka, G. W. and Tuttle, J. V. (1981). Purine nucleoside synthesis, an efficient method employing nucleoside phosphorylases. **Biochemistry** 20(12): 3615-21.

Llaudet, E., Botting, N. P., Crayston, J. A. and Dale, N. (2003). A three-enzyme microelectrode sensor for detecting purine release from central nervous system. **Biosens Bioelectron** 18(1): 43-52.

Macedo, T. C. (1980). Forma indeterminada da Doença de Chagas. . **Jornal Brasileiro de Medicina** 38: 34 - 40.

Mao, C., Cook, W. J., Zhou, M., Koszalka, G. W., Krenitsky, T. A. and Ealick, S. E. (1997). The crystal structure of Escherichia coli purine nucleoside phosphorylase: a comparison with the human enzyme reveals a conserved topology. **Structure** 5(10): 1373-83.

Markert, M. L., Finkel, B. D., McLaughlin, T. M., Watson, T. J., Collard, H. R., McMahon, C. P., Andrews, L. G., Barrett, M. J. and Ward, F. E. (1997). Mutations in purine nucleoside phosphorylase deficiency. **Hum Mutat** 9(2): 118-21.

Miller, R. L., Sabourin, C. L. and Krenitsky, T. A. (1987). Trypanosoma cruzi adenine nucleoside phosphorylase. Purification and substrate specificity. **Biochem Pharmacol** 36(4): 553-60.

Moore, J. D., Hawkins, A. R., Charles, I. G., Deka, R., Coggins, J. R., Cooper, A., Kelly, S. M. and Price, N. C. (1993). Characterization of the type I dehydroquinase from Salmonella typhi. **Biochem J** 295 (Pt 1): 277-85.

Moshier, J. A., Dosescu, J., Skunca, M. and Luk, G. D. (1993). Transformation of NIH/3T3 cells by ornithine decarboxylase overexpression. **Cancer Res** 53(11): 2618-22.

O'Brien, T. G., Megosh, L. C., Gilliard, G. and Soler, A. P. (1997). Ornithine decarboxylase overexpression is a sufficient condition for tumor promotion in mouse skin. **Cancer Res** 57(13): 2630-7.

Prata, A. (2001). Clinical and epidemiological aspects of Chagas disease. **Lancet Infect Dis** 1(2): 92-100.

Provencher, S. W. and Glockner, J. (1981). Estimation of globular protein secondary structure from circular dichroism. **Biochemistry** 20(1): 33-7.

Pugmire, M. J. and Ealick, S. E. (2002). Structural analyses reveal two distinct families of nucleoside phosphorylases. **Biochem J** 361(Pt 1): 1-25.

Savarese, T. M., Harrington, S. and el Kouni, M. H. (1989). Adenine nucleoside phosphorylase and purine nucleoside phosphorylase in *Schistosoma mansoni*. **J Cell Biol** 107(396a).

Schmid, M., Malicki, D., Nobori, T., Rosenbach, M. D., Campbell, K., Carson, D. A. and Carrera, C. J. (1998). Homozygous deletions of methylthioadenosine phosphorylase (MTAP) are more frequent than p16INK4A (CDKN2) homozygous deletions in primary non-small cell lung cancers (NSCLC). **Oncogene** 17(20): 2669-75.

Sifers, R. N. (1995). Defective protein folding as a cause of disease. **Nat Struct Biol** 2(5): 355 - 7.

Stoeckler, J. D. (1984). Purine nucleoside phosphorylase: a target for chemotherapy. Developments in Cancer Chemotherapy. R. J. Glazer. Boca Raton, CRC Press**:** 35 - 60.

Subhi, A. L., Diegelman, P., Porter, C. W., Tang, B., Lu, Z. J., Markham, G. D. and Kruger, W. D. (2003). Methylthioadenosine phosphorylase regulates ornithine decarboxylase by production of downstream metabolites. **J Biol Chem** 278(50): 49868-73.

Takehara, M., Ling, F., Izawa, S., Inoue, Y. and Kimura, A. (1995). Molecular cloning and nucleotide sequence of purine nucleoside phosphorylase and uridine phosphorylase genes from Klebsiella sp. **Biosci Biotechnol Biochem** 59(10): 1987-90.

Tanowitz, H. B., Kirchhoff, L. V., Simon, D., Morris, S. A., Weiss, L. M. and Wittner, M. (1992). Chagas' disease. **Clin Microbiol Rev** 5(4): 400-19.

Teles, R. C., Calderon Lde, A., Medrano, F. J., Barbosa, J. A., Guimaraes, B. G., Santoro, M. M. and de Freitas, S. M. (2005). pH dependence thermal stability of

a chymotrypsin inhibitor from Schizolobium parahyba seeds. **Biophys J** 88(5): 3509-17.

Tello-Solis, S. R. and Hernandez-Arana, A. (1995). Effect of irreversibility on the thermodynamic characterization of the thermal denaturation of Aspergillus saitoi acid proteinase. **Biochem J** 311 (Pt 3): 969-74.

Thomas, P. J., Qu, B.-H. and Pedersen, P. L. (1995). **Trends Biochem Sci** 20: 456 - 9

Walker, J. and Barrett, J. (1997). Parasite sulphur amino acid metabolism. **Int J Parasitol** 27(8): 883-97.

WHO (1993). World development report 1993--investing in health. **Commun Dis Rep CDR Wkly** 3(30): 137.

WHO (1997). Chagas disease. Interruption of transmission. **Wkly Epidemiol Rec** 72(1-2): 1-4.

WHO (2000). Chagas disease, Brazil. Interruption of transmission. **Weekly Epidemiological Record** 75: 153 - 60.

WHO (2002). Control of Chagas Disease. Second report of the WHO Expert Committee., Geneva, World Health Organization.

Williams-Ashman, H. G., Seidenfeld, J. and Galletti, P. (1982). Trends in the biochemical pharmacology of 5'-deoxy-5'-methylthioadenosine. **Biochem Pharmacol** 31(3): 277-88.